

**"OPTIMIZATION OF FLOCCULATION PROCESSES WITH RESPECT TO THE
PHYSICAL PARAMETERS"**

HIS THESIS HAS BEEN ACCEPTED FOR
THE DEGREE OF M.Sc. 1992
AND A COPY HAS BEEN DEPOSITED IN THE
UNIVERSITY LIBRARY

BY

OBOTE/PAITO B.SC., M.SC.(E.H.E.) CANDIDATE

A THESIS SUBMITTED IN PARTIAL FULFILMENT FOR THE DEGREE OF MASTER
OF SCIENCE IN ENVIRONMENTAL HEALTH ENGINEERING IN THE UNIVERSITY
OF NAIROBI.

NOVEMBER, 1992.

FOR USE IN THE LIBRARY

UNIVERSITY OF NAIROBI LIBRARY

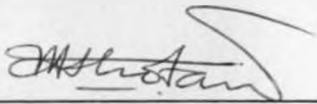


0100010 8

UNIVERSITY OF NAIROBI
LIBRARY

DECLARATION

THIS THESIS IS MY ORIGINAL WORK AND HAS NOT BEEN PRESENTED FOR A DEGREE IN ANY OTHER UNIVERSITY.



DATE: 30/11/52

OBOTE PAITO
(CANDIDATE)

THIS THESIS HAS BEEN SUBMITTED FOR EXAMINATION WITH MY APPROVAL AS UNIVERSITY SUPERVISOR.



DATE: 30/11/52

DR. M. M. NDEGE
LECTURER, DEPARTMENT OF CIVIL ENGINEERING,
UNIVERSITY OF NAIROBI.

DEDICATION

To my spouse, Gertrude, and late son, Nathan, for their love and patience.

TABLE OF CONTENTS

	Page
DECLARATION	ii
DEDICATION	iii
ACKNOWLEDGEMENTS	viii
PRINCIPLE SYMBOLS AND NOTATIONS	ix
ABSTRACT	x
CHAPTER ONE	
INTRODUCTION	1
1.1 Coagulation-Flocculation in Water Treatment	1
1.2 Theory of Coagulation-Flocculation	2
1.2.1 Nature of Colloids	2
1.2.2 Mechanisms of Destabilization	3
1.2.3 Transport Mechanisms	4
1.3 Principles of Coagulation-Flocculation	5
1.4 Coagulation-Flocculation Practice	8
1.4.1 Choice of Coagulants/Flocculant Aids	8

	Page
1.4.2 Coagulation-Flocculation Process Design and Control .	10

CHAPTER TWO

LITERATURE REVIEW	14
2.1 Theoretical Developments in the Physical Aspects of Flocculation	14
2.1.1 Brownian Diffusion Model	14
2.1.2 Laminar flow Model	15
2.1.3 Turbulent Flow Models	16
2.1.4 Validity of the Kinetic Models	19
2.2 Previous Experimental and In-plant Studies on the Physical Aspects of Flocculation	20
2.3 Objectives of Study	28

CHAPTER THREE

DESIGN OF EXPERIMENTAL INVESTIGATION	30
3.1 Scope of Study	30
3.2 Methodology	30
3.3 Design of Mixing Equipment	31
3.4 Equipments and Materials	35
3.5 Reagents/Sample Preparation	36
3.6 Experiments	38
3.6.1 General Principles	38
3.6.2 Rapid Mix Process	38
3.6.3 Preliminary Experiments	39
3.6.4 Final Experiments - Optimization	42

CHAPTER FOUR

	Page
RESULTS, ANALYSIS AND DISCUSSIONS OF RESULTS	44
4.1 Experimental Data	44
4.2 Analysis of Results	57
4.3 Discussions of Results	63
4.3.1 Experimental Conditions	63
4.3.2 Results	64
4.3.3 Practical Applications of Results	66

CHAPTER FIVE

CONCLUSIONS AND RECOMMENDATIONS	68
5.1 Conclusions	68
5.2 Recommendations	69
REFERENCES	71

APPENDIX 1

DATA FROM THE FINAL EXPERIMENTS	75
---	----

APPENDIX 2

RESULTS OF PRELIMINARY EXPERIMENTS	85
--	----

ACKNOWLEDGEMENTS

I owe this work to AMREF - Environmental Health Unit (E.H.U.), who met the full financial requirements for the work. I deeply appreciate the physical assistance extended by E.H.U. towards this work.

Special thanks go to my supervisors, Dr. M. M. Ndege and Dr. F. Otieno, lecturers in the department of civil engineering, University of Nairobi, for their constructive criticisms, guidance, encouragements, and material assistance which lightened my work.

I appreciate the cooperation of Mr. S. Ng'ang'a and Mr. J. Thiongo, technicians in the public health engineering laboratory, University of Nairobi, during my laboratory investigation. My classmates, Mr. S. O. Omol and Mr. A. Mabonga, were always available to discuss my work.

I am grateful to the E.H.U. staff, Eng. M. N. Kariuki, Mr. J. Thuku, Mr. V. Njuguna, Ms. M. Munano, Mr. G. M. Muhanji, Mrs. A. Masila, and Mrs. E. Wairagu for their great concern and cooperation offered to me during my study. I am particularly thankful to Mr. Gilbert M. Muhanji for his commitment to help me edit and print my work.

Finally, I wish to express my gratitude to Ms. Anjeline Ayuya of the University of Nairobi for the typing services she rendered and to all those who assisted me in one way or the other during the study period.

PRINCIPLE SYMBOLS AND NOTATIONS

α	Collision - aggregation ratio
D	Diffusion coefficient
E	Power input per unit mass
dv/dz	Laminar velocity gradient
G	Root mean square velocity gradient
G_{opt}	Optimum G
G.T	Dimensionless product of G and retention time
k	Boltzmann's constant
n	Number concentration of particles
N	Residual turbidity
N_0	Raw water turbidity
NTU	Nephelometric turbidity unit
N_{xy}	Collision frequency between x,y particles
ϕ	Floc volume concentration
RPM	Revolutions per minute
t	Temperature (absolute, °C)
T	Retention time (seconds, minutes)
T_{opt}	Optimum T
μ	Dynamic viscosity
\bar{U}^2	mean square velocity fluctuation
ν	Kinematic viscosity

ABSTRACT

Conventional water treatment usually include coagulation - flocculation processes. Flocculation is influenced by several factors, both physical and chemical. The study presents: short notes on coagulation - flocculation theory, principles, and practice; a brief review of literature on the physical aspects of flocculation with special reference to flocculation kinetics. A rational approach for optimizing the physical parameters of flocculation is presented. The optimum combination of velocity gradient, G , and time of mixing, T , has been suggested for raw water turbidities and temperatures normally encountered in water and their possible applications in process design and control discussed.

At a given temperature, the optimum G value, G_{opt} , and the optimum power function, $G_{opt} \cdot T_{opt}$, have linear relationships with the logarithm of the raw water turbidity value. There is also a linear relationship between the logarithms of G_{opt} and T_{opt} at all temperatures and turbidity values. For a given turbidity, optimum G and T values are higher at lower temperatures while for a given temperature the optimum values are higher at lower turbidity values.

Key words: Water Treatment, Coagulation - Flocculation, Gentle mix, Velocity Gradient, Retention Time, Turbidity, Temperature, Optimization.

CHAPTER ONE

INTRODUCTION

1.1 Coagulation-Flocculation in Water Treatment

Coagulation-flocculation followed by clarification is, by far, the most widely used process to remove suspended and colloidal particles from water. The process usually begins with rapid dispersal of chemical coagulant (mostly salts of aluminium or iron) into the raw water stream followed by gentle mixing. The process is influenced by many factors like the type of chemical(s) used, the raw water characteristics (both chemical and physical), and the desired level of treatment.

All natural water sources contain some form of impurities which are mostly solids in nature. Such impurities comprise suspended and/or dissolved organic and/or inorganic matter and numerous biological forms. Most suspended materials are comprised of colloids (size range: 10^{-6} to 10^{-3} mm) and materials in solution (smaller than 10^{-6} mm)[6]. The impurity content of water is described by various water quality parameters, narrative or numerical, relating to physical, chemical, or biological characteristics.

Major water treatment processes are meant to achieve solids-liquid separation. Solids content of water is described by physical parameters like turbidity, suspended solids, dissolved solids, and colour. The levels of these parameters vary widely (periodically and

spatially) with wide ranging effects on treatment processes; this has made the design and operation of water treatment systems difficult. Most of these processes are also affected by temperature variations.

Applications of coagulation-flocculation process in water purification date back to several centuries B.C. [17] when natural coagulants were added to water in various forms, in most cases without mixing. The systematic use of polyvalent inorganic salts as coagulants started in the closing years of the last century [14] when the laws governing their action were established. Studies of coagulation-flocculation kinetics date from the early years of this century when Von Smoluchowski [31] derived the basic expressions for particles collision; since then, many studies had been conducted culminating in the modern theory and practice of coagulation-flocculation.

1.2 Theory of Coagulation-Flocculation

1.2.1 Nature of Colloids

Colloids, because of their small sizes, possess a colossal surface area to mass ratio giving rise to an overriding influence of surface phenomena thus their ability to exist as stable dispersions; the hydrodynamic effects are negligible in this case [6]. Such surface phenomena include the effects of the surface charge and the degree of hydration (or solvation) of the surface layer. Other phenomena like thermal convection, molecular and ionic bombardment serve to maintain particles in effectively permanent suspension.

Surface charges originate from [6]:

- lattice imperfections at the solid surface;
- selective adsorption of ions to the solid's surface;
- chemical reactions at the surface of the solid. Here the nature of the charge is pH dependent i.e. positive at low pH and negative at high pH.

Most colloids in water carry a negative charge but a colloidal dispersion does not have a net charge [25]. The primary charges on the particles are countered by charges in the aqueous phase resulting in an electrical double layer at every interface between the solid and water. The interaction between the electrical double layers leads to mutual repulsion between particles; this repulsion is opposed by the universal Van der Waal's force of attraction.

Depending on the degree of hydration, colloids are referred to as hydrophobic or hydrophilic inferring low or high degree of hydration respectively. The extensive hydration of hydrophils has the effect of a physical barrier to destabilization [6].

1.2.2 Mechanisms of Destabilization

There are basically four mechanisms of destabilization:

- Compression of the electrical double layer: by increasing the ionic strength of the solution, the double layer is compressed thereby reducing the range of interparticle repulsion. Transition from stability to destabilization is over a narrow range of concentration and an excess of the indifferent electrolyte has no effect [6]; also particle concentration does

not affect the amount of coagulant required for destabilization.

- Specific adsorption mechanism: specific adsorption of counter-ions to the colloid surface reduces the effect of surface charge hence destabilization. An excess of coagulant would result in charge reversal and subsequent restabilization [6].
- Bridging mechanism: as a result of pronounced polymerization due to hydrolysis, metal coagulants form polynuclear species which adsorb to particles thus forming a bridge between adjacent particles thereby promoting destabilization; this is also applicable to polyelectrolytes [15]. An overdose of coagulant may result in restabilization.
- Precipitate enmeshment: under certain conditions, metal coagulants in aqueous solutions form metal hydroxide precipitates which serve to enmesh colloids thus effecting destabilization. An overdose of coagulant has no effect [15].

1.2.3 Transport Mechanisms

There are three ways in which particles in suspension can be brought into contact:

- by Brownian motion (thermal agitation) resulting in perikinetic flocculation. This is a naturally random process and it is only effective for particle size smaller than the Kolmogoroff microscale [15].
- by agitation and fluid motion resulting in orthokinetic flocculation. Here velocity gradient is induced in the fluid by hydraulic or mechanical agitation; the velocity gradient is

to set up relative velocities between particles thereby providing opportunity for contact [15].

- by differential settling of particles. In a suspension where there is a wide range of particle size, bigger particles would settle faster than smaller particles thereby causing velocity gradients between particles. This mechanism is pronounced in suspensions with high solids concentration [15].

1.3 Principles of Coagulation-Flocculation

Coagulation and flocculation are often used interchangeably in many areas of chemical engineering practice [25], but in water treatment practice these terms are recognized to be separate and distinct although complementary. Bratby [6] has defined the processes as follows:

- Coagulation is the process whereby a given suspension or solution is destabilized.
- Flocculation is the process whereby destabilized particles formed as a result of coagulation are induced to come together, make contact and thereby form larger agglomerates.

The overall process of coagulation-flocculation is controlled by three sub-processes as shown schematically in Fig. 1.1 below [23]; each of these sub-processes depend on many factors as discussed below. The rate of achieving steady state size distribution as well as the form of the size distribution depends on the hydrodynamics of the system and the chemistry of the coagulant-particulate interactions.

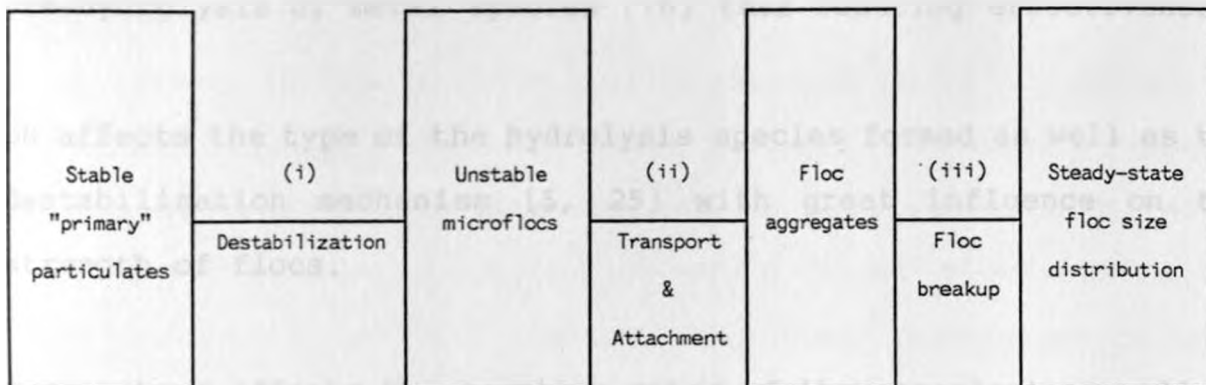


Fig.1.1 Subprocesses in coagulation-flocculation (Montgomery,[23])

Destabilization

This process is accomplished in the rapid mix stage. The nature of the microflocs formed markedly influence the subsequent flocculation process and as such the rapid mix process is considered possibly the most important in coagulation-flocculation [6]. The efficiency of destabilization depends on: the intensity and duration of mixing, the nature and dosage of coagulant, the coagulant feed concentration, the nature and concentration of colloids, pH, and temperature. Very high mixing intensity can lead to breakup of the microflocs yielding stable particles [32] while low intensity may not provide adequate collision opportunity. Extended mixing at high intensity can lead to floc erosion yielding stable particles.

Coagulant dosage affects the characteristics of the hydrolysis species formed and thus the nature of the flocs [6]. Different types of coagulants give different types of flocs.

Dilute coagulant solution disperse more rapidly and uniformly than concentrated solutions [19] but very dilute solutions may cause

pre-hydrolysis of metal species [18] thus reducing effectiveness.

pH affects the type of the hydrolysis species formed as well as the destabilization mechanism [5, 25] with great influence on the strength of flocs.

Temperature affects the reaction rates of the coagulant as well as the diffusivity of the particulates and hence the rate of formation of microflocs which result from perikinetic flocculation.

Transport and Attachment

The effectiveness of this process depends on: the intensity and duration of mixing, the nature and concentration of the microflocs, and the rapid mix condition in the previous step.

High velocity gradients result in smaller floc sizes due to continuous breakdown of larger flocs; hence for a given velocity gradient there is a limiting mixing time beyond which there is no further growth in floc sizes [6].

Surface chemistry, and hence the nature of the forces holding the flocs together, depends on the coagulant species formed as well as the mechanism of destabilization that came into effect.

Higher concentrations of microflocs require lower velocity gradients while very low concentrations may require the use of flocculant aid for effective flocculation [6].

Floc Breakup

This refers to the erosion and disruption of floc aggregates subjected to unequal shearing forces during the transport process. It depends on the mixing intensity and the nature and concentration of flocs; high floc concentration would favour floc erosion. At steady-state floc size distribution, the growth and disruption rates of flocs are roughly equal [26].

1.4 Coagulation-Flocculation Practice

1.4.1 Choice of Coagulants/Flocculant Aids

There are many types of coagulant/flocculant aids which can be classified as organic or inorganic, natural or synthetic, and ionic (cationic/anionic) or non-ionic.

The most widely used coagulants are based on aluminium or iron salts [6]. Synthetic products such as cation polyelectrolytes are also used, but mostly in combination with metal salt [14]. The majority of flocculant aids are synthetic (polyacrylamides or polyamines) [14] though the use of organic aids is subject to national regulations; coagulant aids are not commonly used in Kenya. The common inorganic aids are activated silica, certain types of clay, powdered activated carbon [6].

The choice of coagulant/flocculant aids together with their sequence of addition is done after flocculation tests on the water to be treated have been done. Since many factors affect the coagulation-flocculation process, the assessment of the optimum

conditions for the overall process requires a testing procedure which can control as many parameters as possible while others are being studied; the universally adopted experimental procedure is the jar test [6].

In performing jar tests, two factors are of importance i.e. the performance criteria to be applied and the desired level of performance [6].

The performance criteria applied depends on the water constituents. These constituents mostly comprise those giving rise to turbidity and/or colour thus making turbidity and colour the most common criteria used in water testing [6]; they are also easy to determine. Other factors that affect the choice of performance criteria are the treatment processes used and the desired quality of treated water.

The level of performance can be expressed in terms of percentage removal or residual level of the given parameter. Bratby [6] recommended the former method for analyzing a particular water for design purposes and the latter method for research application.

1.4.2 Coagulation-Flocculation Process Design and Control

Coagulation Process

Coagulation takes place in the rapid mix stage. Rapid mix is achieved in pumps, baffled channel, hydraulic jump, in-line blenders, impeller or propeller mixers. The design parameters for rapid mix units are the velocity gradient, G , and the mixing time, T , [27]. Other factors considered in design are the reactor geometry, flexibility of operation, flow and velocity gradient distribution in the reactor, and chemical handling.

Process control is concerned with chemical dosage and pH control to suit the incoming raw water; velocity gradient and retention time are rarely factors of control in the routine operation of rapid mix process [12]. Chemical requirements are determined from the jar tests performed whenever there is a major variation in water quality. The jar test procedure should correspond to the full plant conditions [27].

Flocculation Process

Flocculation takes place in the gentle agitation (transport) stage. Gentle mix is achieved through hydraulic or mechanical means. Hydraulic mixers include: baffled chambers, spiral flow, solids contact blanket, fluidized bed, and gravel bed flocculators while mechanical mixers include: rotating blades, reciprocating blades, and diffused air flocculators. The choice of flocculator (and rapid mixer) is closely linked with the choice of separation process used in the next stage of treatment. Other factors influencing choice are related to funding, operation and maintenance, availability of land, operation flexibility, and plant capacity.

The design parameter for flocculators is the dimensionless product GT (velocity gradient \times mixing time) [15, 27]. Other factors considered in flocculator design are: distribution of velocity gradient and time of mixing in the reactor, compartmentalization, inlet and outlet system.

Tapered mixing and compartmentalization were shown to greatly improve efficiency of the overall process [3, 6]. Proper design of inlets and outlets to ensure uniform flow distribution and collection reduces short circuiting; compartmentalization also minimizes short circuiting.

Process control in flocculators is concerned with the physical parameters i.e. velocity gradient and mixing time [12] though retention time in a reactor is usually fixed. The need for adjustments is realized when the flocculated water quality is unacceptable.

In general, coagulation-flocculation process control is a trial-and-error procedure because the information obtained from jar-test experiments bear little relevance to plant operation [2] and as such the conditions found satisfactory may not be the optimum.

Methods of Design

There are three methods used in design i.e. empirical formulation, rational design, and rule-of-thumb procedure.

In empirical formulation, the design data is got either from existing plant treating water of similar quality or from pilot plants/laboratory studies. Fundamental theory of flocculation is required to transfer empirical data obtained from one system to another [2]. Empirical method of design is still the most widely used especially for big plants [6].

The rational design method is based on theoretical formulation of flocculation kinetics and usually combined with experimental studies from which rational design criteria are developed. It is essential to conduct pilot plant studies to evaluate the new design [2]. The design depends on the kinetic equation used.

In the rule-of-thumb procedure, the design criteria are developed from long experience in operation of flocculation facilities. Design using this method is very subjective but because of high costs and lengthy testing procedures involved in pilot plant studies, design of relatively small plants are based on rule-of-thumb procedure [6]. The design criteria mostly quoted for alum coagulation [15] is the GT value between 10,000 and 100,000 while other publications [33, 23] recommend G and T values.

Conclusion

The design and control of flocculation process is based on the physical characteristics of flocculation and is still largely a trial-and-error procedure [2]. The aim of this study is, therefore, to quantify the relationships between these physical parameters of

flocculation in view of more direct applications in optimum process design and control.

LITERATURE REVIEW

2.1 Theoretical Developments in the Physical Aspects of Flocculation

Early studies of flocculation kinetics focused on determining the frequency of collision between suspended particles in a fluid medium (1). The early theories were derived by Von Smoluchowski (2) who derived the basic expressions for collision frequencies for laminar flow regimes; other models for turbulent regimes were developed in later studies.

2.1.1 Smoluchowski Diffusion Model

The rate of collision between diffusing particles was determined by Smoluchowski (3) who assumed a diffusional flux of particles towards a stationary single particle. He derived the following equation for perikinetic flocculation:

$$R_{ij} = 4\pi(D_i + D_j)R_j n_i n_j \quad (2.1)$$

R_{ij} = collision frequency per unit volume between particles of

size i and j

D_i, D_j = diffusion coefficient ($D_i + D_j$)

R_i, R_j = collision radius ($R_i + R_j$)

n_i, n_j = respective number concentrations of i and j particles

CHAPTER TWO

LITERATURE REVIEW

2.1 Theoretical Developments in the Physical Aspects of Flocculation

Most studies of flocculation kinetics focussed on determining the frequency of collision between suspended particles in idealized system [3]. The early theories were developed by Von Smoluchowski [31] who derived the basic expressions for collision frequencies under Brownian motion and laminar flow regimes; other models for turbulent regimes were developed in later studies.

2.1.1 Brownian Diffusion Model

The rate of collision between diffusing particles was determined by Von Smoluchowski [31] who assumed a diffusional flux of particles in a radial direction towards a stationary single particle. He derived the following equation for perikinetic flocculation:

$$N_{ij} = 4\pi D_{ij} R_{ij} n_i n_j \quad \text{--- (2.1)}$$

where N_{ij} = Collision frequency per unit volume between particles of radius R_i and R_j ;

D_{ij} = mutual diffusion coefficient ($D_i + D_j$);

R_{ij} = collision radius ($R_i + R_j$);

n_i, n_j = respective number concentrations of i and j particles.

The mutual diffusion coefficient given above is only valid for particles whose diffusional motions are completely independent. The individual diffusion coefficient is given by [25]:

$$D_i = kt/(6\mu R_i) \text{ --- (2.2)}$$

where k = Boltzmann's constant;

t = absolute temperature;

μ = dynamic viscosity.

2.1.2 Laminar flow Model

The collision frequency between particles under laminar flow regime was determined by Von Smoluchowski [31] who assumed that particles would move along streamlines developed in laminar flows. He derived the following equation for orthokinetic flocculation in laminar flow regime:

$$N_{ij} = 4/3 n_i n_j R_{ij}^3 dv/dz \text{ --- (2.3)}$$

where N_{ij} = collision frequency per unit volume between particles of radius R_i and R_j ;

n_i, n_j = number concentration of particles i, j ;

R_{ij} = collision radius ($R_i + R_j$);

dv/dz = velocity gradient in laminar flow.

Equation (2.3) is considered to be the basic equation describing orthokinetic flocculation [31].

2.1.3 Turbulent Flow Models

Two basic turbulent flow models were developed by Camp and Stein [9] and Argaman and Kaufman [3].

Camp and Stein [9] observed that velocity gradient in a turbulent fluid system changes from point to point and suggested the use of the average

value of velocity gradient in equation (2.3) which would be more useful in explaining turbulent flocculation. Using Stoke's theory they related the energy input to the system to the resulting root mean square velocity gradient as:

$$G = (E/\nu)^{1/2} \quad - - - - - (2.4)$$

where G = root mean square velocity gradient (s^{-1});

E = power input per unit mass ($Nms^{-1} kg^{-1}$);

ν = kinematic viscosity of fluid (m^2s^{-1}).

They then substituted G for the laminar velocity gradient in equation (2.3) and the resulting collision frequency for turbulent orthokinetic flocculation was:

$$N_{ij} = 4/3 n_i n_j R_{ij}^3 G \quad - - - - - (2.5)$$

Equation (2.5) is considered to be the basic expression for turbulent orthokinetic flocculation [26]. Its working form at steady-state in a continuously stirred reactor is given by:

$$n_1/n_2 = 1 + K\phi GT \quad - - - - - (2.6)$$

Where: ϕ = floc volume concentration;

K = constant depending on nature and size of suspension;

n_1, n_2 = concentration of primary particles in influent, effluent;

T = mean residence time.

Argaman and Kaufman [3] based their model on the hypothesis that particles suspended in turbulent fluid experience a random motion which may be described by a diffusion coefficient; they expressed the coefficient in terms of the energy spectrum describing the distribution of kinetic energy in fluid motions of various frequencies. The resulting flocculation equation was:

$$N_{1F} = 4\pi K_S R_F^3 n_1 n_F \bar{U}^2 \quad - - - (2.7)$$

where N_{1F} = collision frequency per unit volume between primary particles (1) and floc particles (F);

R_F = radius of floc particles ($R_F \gg R_1$);

n_1, n_F = respective number concentration of primary particles, floc particles;

\bar{U}^2 = mean square velocity fluctuation;

K_S = a proportionality factor expressing the effect of the turbulence energy spectrum on the diffusion coefficient.

K_S is a constant for a particular turbulence field and particle size.

Based on experimental measurements, they further related \bar{U}^2 to G as follows:

$$\bar{U}^2 = K_p G \quad - - - - - (2.8)$$

where K_p is a performance parameter characterizing the stirring arrangement.

The authors [3] introduced the importance of floc breakup in equation (2.7) by adding a breakup term as follows:

$$dn_1/dt = -\alpha N_{1F} + B (R_F/R_1)^2 n_F \bar{U}^2 - - - - - (2.9)$$

where dn_1/dt = the rate of release of primary particles;

α = aggregation - collision ratio;

B = breakup constant

The solution to this equation at steady-state in a continuously stirred reactor with one compartment was presented in the simplified form below:

$$n_1/n_2 = (1 + K_A GT)/(1 + K_B G^2 T) - - - - - (2.10)$$

where n_1, n_2 = respective concentration of primary particles in influent, effluent;

T = mean retention time;

$K_A = K_S K_P K_F$ = aggregation constant;

$K_F = 3\alpha\phi$ = flocculation constant;

ϕ = floc volume fraction;

K_B = general breakup constant

The root mean square fluctuating velocity, $(\bar{U}^2)^{1/2}$, was shown to be proportional to the third-root of power input per unit mass, E [10]; hence from equation (2.7), the collision frequency is a function of $E^{2/3}$. Meanwhile from equation (2.10) the product GT can be regarded as an adequate design parameter for small values of G [3].

2.1.4 Validity of the Kinetic Models

Equation (2.5) has been considered as the basic expression describing turbulent orthokinetic flocculation [22] and has found long standing acceptance and usage in design and studies of flocculation process [20]. The equation has, however, been criticized several times since its inception.

- Mark [20] showed that the simple transformation of the dissipation function used by Camp and Stein [9] to derive the equation is not applicable to orthokinetic flocculation and that the conceptualization of "absolute velocity gradient" and a "root mean square velocity gradient" is fundamentally incorrect in that a three-dimensional flow would be represented by a single two-dimensional flow.
- Argaman and Kaufman [3] noted that G does not take into account the length and time scale over which the turbulent velocity fluctuations occur given that the velocity gradient of a given length scale does not contribute significantly to the collision of particles much smaller or much larger than this scale; equation for laminar condition (equation 2.3) cannot therefore be used to describe conditions in turbulent regime.
- Cleasby [10] showed that G is only valid for particles smaller than the microscale and as such may be applicable to rapid mixing of short duration (less than 30 seconds) during which the aggregation of such small particles take place. He further observed that since the important turbulent eddies causing flocculation are larger than the microscale, process effectiveness should be independent of temperature thus taking

$E^{2/3}$ as a more appropriate flocculation parameter than G for common flocculation practice.

- Bratby [6] observed that equation (2.5) does not take into account floc breakup and hence cannot describe fully the flocculation process since floc breakup is a very important factor in flocculation process.

The validity of equation (2.10) was demonstrated experimentally by Argaman and Kaufman [3] while Argaman [2] used the values of K_A and K_B obtained from a pilot plant to successfully predict the performance of a full scale plant. The inadequacy of equation (2.10) was pointed out by Bratby [6]; from flocculation tests performed he found out that the breakup constant, K_B , does not remain constant for each G value thus indicating the inadequacy of the breakup mechanism assumed.

Despite identifying \bar{U}^2 and its spectrum as the only energy parameters directly affecting flocculation process, Argaman and Kaufman [3] still introduced G into the flocculation equation because G is easy to estimate and it has been widely accepted by sanitary engineers [10].

2.2 Previous Experimental and In-plant Studies on the Physical Aspects of Flocculation

The physical parameters of flocculation process which are widely investigated are the velocity gradient (G) and the flocculation period (T); another factor of great significance is the reactor geometry. Meanwhile the physical parameters of water quality mostly used in flocculation studies are turbidity, colour, and temperature.

Many studies have been carried out to evaluate the effects of G and T on the flocculation process under various conditions.

Kawamura [19] investigated the effect of G on residual turbidity when water of varying quality and alum dose of 17 to 100 mg/l were used while T was held constant at 15 minutes. The optimum G was found to decrease with increasing dose. This may be because at higher alum dose weaker flocs are formed and thus high G values would lead to excessive floc breakup; also at high alum dose the sweep mechanism of destabilization becomes pronounced due to increased solid content thus reducing the need for external mixing. The author also found that G value of 50 sec^{-1} apply to a wide range of flocculation processes and values in excess of 50 sec^{-1} lead to decreased effectiveness. Settled residual turbidity was the measure of performance.

Argaman and Kaufman [4] using a continuous flow bench scale reactor observed that given T, performance increases, almost linearly, with G until a maximum value is reached beyond which increase in G is detrimental. The optimum G values observed were a function of T and varied from about 30 sec^{-1} for T = 48 minutes to 100 sec^{-1} for T = 4 minutes; the alum dose used was 25 mg/l and performance was determined by settled residual turbidity measurements.

Rafael and Letterman [28] using bench scale batch reactors performed various tests on 100mg/l Kaolin Clay suspension (about 30NTU) under different rapid mix condition and/or alum dose as follows:- Series A: rapid mix at 800 sec^{-1} for 3 minutes and alum dose of 10 mg/l;

series B: rapid mix at 500 sec.^{-1} for 5 minutes and alum dose of 10 mg/l; series C: rapid mix at 800 sec.^{-1} for 3 minutes and alum dose of 25 mg/l; and series D: rapid mix at 800 sec.^{-1} for 3 minutes and alum dose of 50 mg/l. The major objective was to evaluate the influence of the alum dose and retention time on the optimum velocity gradient. They made the following observations:

- For G values greater than 100 sec.^{-1} , performance increases with T until a maximum is reached beyond which performance decreases. For G values of 25 sec.^{-1} and below, no maximum performance was observed (figure 2.1).
- For a given T there exists an optimum G value. According to figure (2.2), this optimum G value decreases with T i.e. from 40 sec.^{-1} at T = 10 minutes to 20 sec.^{-1} at T = 120 minutes. Performance was also observed to increase with T, however, the rate of increase diminishes after T of about 20 minutes; the residual turbidity for T of 20, 30 and 40 minutes was about 1.5 NTU. Figure (2.2) was derived from figure (2.1) and other similar graphs.
- Figure (2.3), series A and B, indicates that rapid mix conditions have little, if any, effect on the relationship between the optimum G and T. Also, curves for series A and B, C, and D were found to be parallel indicating that the relationship between the optimum G and T depended on the alum dose only; the higher the alum dose the lower the optimum G value. Figure (2.3) was derived from figure (2.2) and other similar graphs.

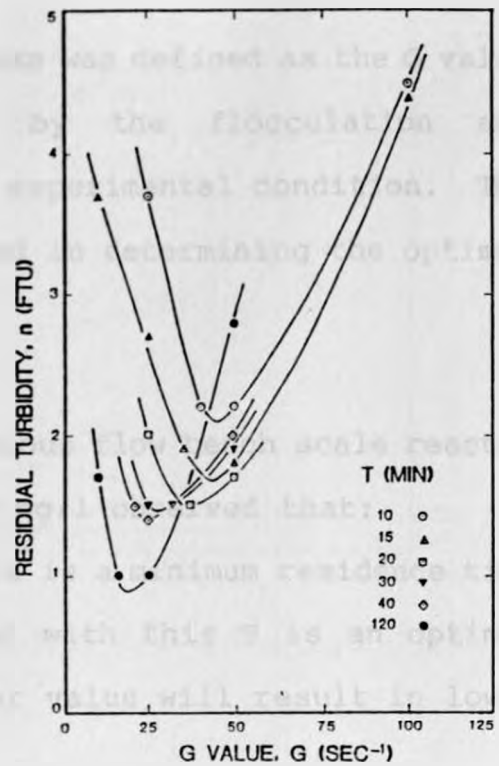
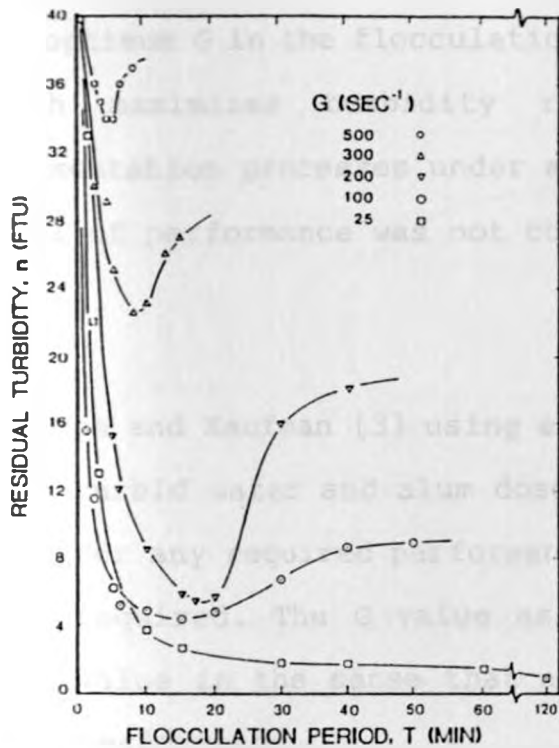


Fig.2.1 Residual turbidity versus T for several G values -series A (Rafael and Letterman [28]). Fig.2.2 Residual turbidity versus G for several T values series A (Rafael and Letterman [28]).

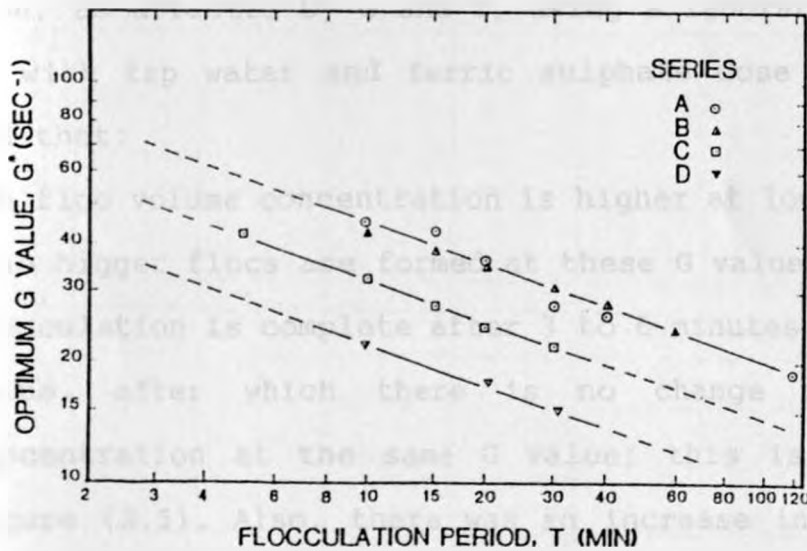


Fig.2.3 Optimum G Versus T (Rafael and Letterman [28])

The optimum G in the flocculation process was defined as the G value which maximizes turbidity removal by the flocculation and sedimentation processes under a given experimental condition. The level of performance was not considered in determining the optimum G .

Argaman and Kaufman [3] using a continuous flow bench scale reactor with turbid water and alum dose of 25 mg/l observed that:

- For any required performance there is a minimum residence time required. The G value associated with this T is an optimum value in the sense that any other value will result in lower performance.
- For a given T , performance increases with the degree of compartmentalization.

These conclusions were drawn from Figure (2.4) which is based on equations (2.9 and 2.10) and supported by the experimental results.

Camp [7] studied the characteristics of flocs formed under rapid mix condition, as affected by G and T , using a laboratory scale batch reactor with tap water and ferric sulphate dose of 15 mg/l; he observed that:

- the floc volume concentration is higher at lower G values and also bigger flocs are formed at these G values.
- flocculation is complete after 3 to 6 minutes, depending on G value, after which there is no change in floc volume concentration at the same G value; this is illustrated in Figure (2.5). Also, there was an increase in floc size, for each fraction of floc volume, with time of mix, even after

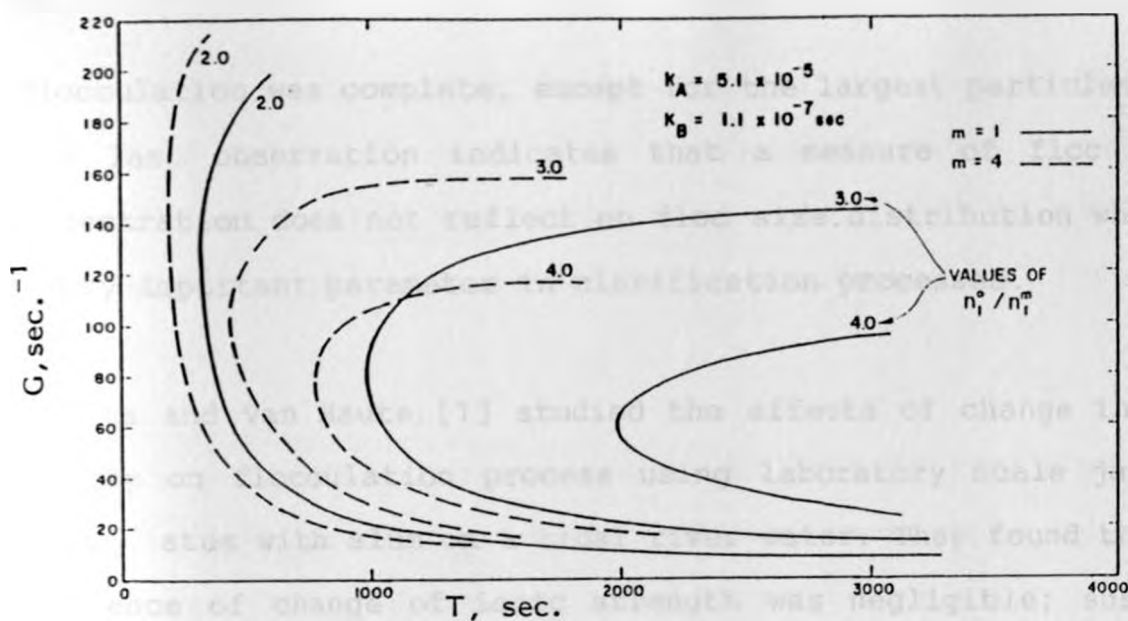


Fig.2.4 Relation of performance to G, T , and m (Rafael and Letterman [28]).

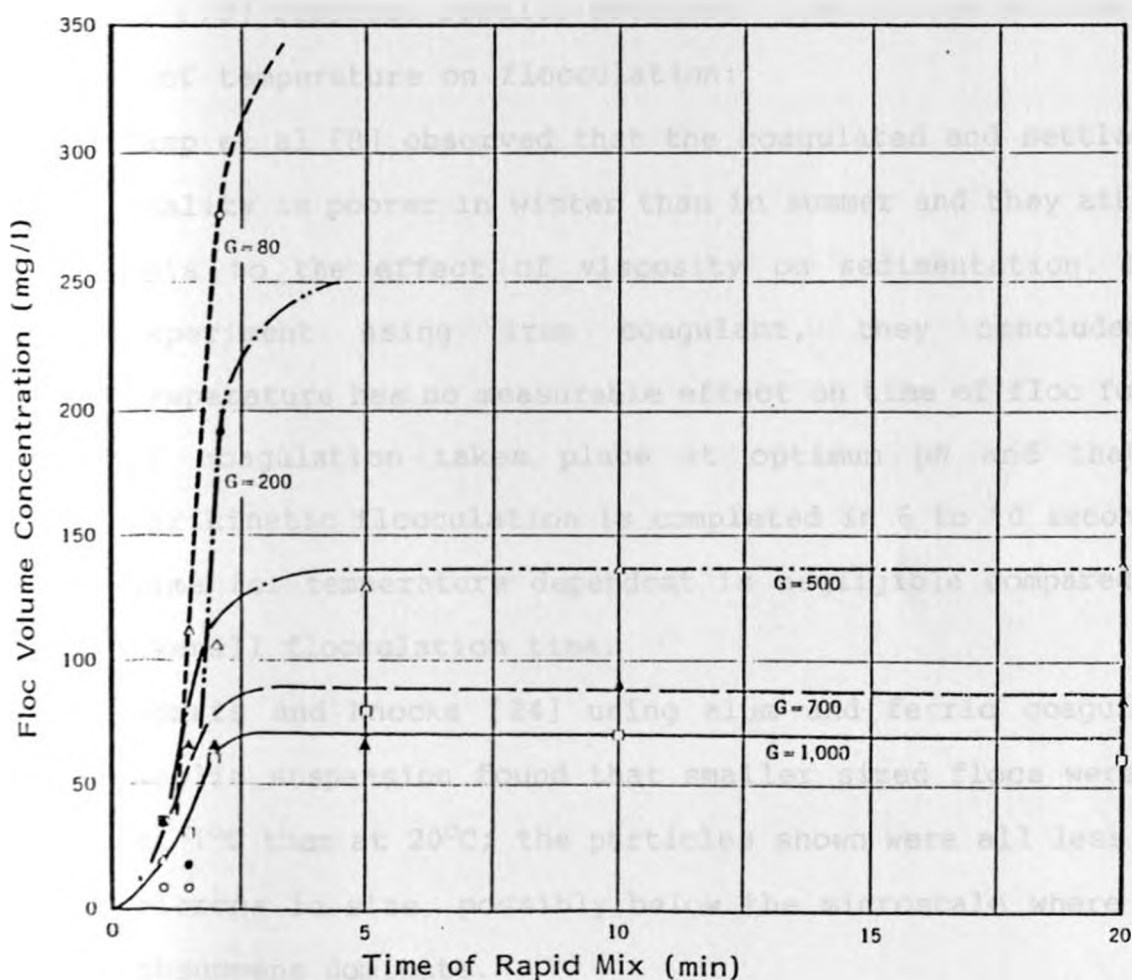


Fig.2.5 Effects of time of rapid mix on floc volume concentration (Camp [7]).

flocculation was complete, except for the largest particles. This last observation indicates that a measure of floc volume concentration does not reflect on floc size distribution which is a very important parameter in clarification processes.

Alaerts and Van Haute [1] studied the effects of change in water quality on flocculation process using laboratory scale jar test apparatus with alum on a tidal river water. They found that the influence of change of ionic strength was negligible; suspended solids concentration proved to be a decisive control parameter in flocculation.

Cleasby [10] reported results obtained from various studies on the effect of temperature on flocculation:

- Camp et al [8] observed that the coagulated and settled water quality is poorer in winter than in summer and they attributed this to the effect of viscosity on sedimentation. From an experiment using iron coagulant, they concluded that temperature has no measurable effect on time of floc formation if coagulation takes place at optimum pH and that since perikinetic flocculation is completed in 6 to 10 seconds, the time for temperature dependent is negligible compared to the overall flocculation time.
- Morris and Knocke [24] using alum and ferric coagulants on kaolin suspension found that smaller sized flocs were formed at 1°C than at 20°C; the particles shown were all less than 50 microns in size, possibly below the microscale where viscous phenomena dominate.

Treweek [30] optimized flocculation time prior to direct filtration using alum and a polymer aid in a laboratory batch reactor. He observed that within the temperature range 4.5 to 19°C, the physio-chemical process appears to be unaffected by temperature variations.

The importance of turbulence field developed in the reactor was demonstrated by Argaman and Kaufman [3] who used "stake and stator" stirrer and "turbine" stirrer. They observed that for a given G value, the "stake and stator" stirrer consistently performed better than the "turbine" stirrer; this was attributed mainly to the higher paddle performance factor, K_p (equation 2.7) in the reactor. The floc size seemed not to be affected by stirrer type [3].

The importance of rapid mix process in coagulation-flocculation in relation to the raw water turbidity was demonstrated by Mhaishalkar et al [22] who treated Kaolin suspension with alum in a bench scale reactor to obtain the optimum combination of velocity gradient (G^*) and time of rapid mix (T^*) for turbid waters. The study established that G^* and T^* have a great influence on the flocculation process and that their optimum combination is dependent on the turbidity of the suspension; the results are shown in table 2.1 below:

Table 2.1 Optimum G and T for Rapid Mix Process (Mhaishalkar et al, [22])

Turbidity (NTU)	Optimum G (sec. ⁻¹)	Optimum T (sec.)	G.T.
30	750	40	30,000
120	550	60	33,000
480	450	90	40,500

Conclusions From Literature

Theoretical developments in flocculation kinetics have not yet produced equations that can accurately define flocculation process (section 2.1.4) and thus their application in design is not definite; determination of the values of kinetic variables is also tedious. It is therefore important to correlate flocculation design parameters to pertinent water quality parameters for purposes of design and operation of flocculators.

The limitation of most of the experimental studies mentioned above is the use of a fixed value of G or T throughout the experiments; also, the performance level was not fixed thus making application of results difficult. For a given suspension, each T value has a corresponding optimum G value but for any desired performance there is a minimum T value to achieve it; it is therefore important to optimize both G and T for a given water to facilitate optimum design of flocculation units.

2.3 Objectives of Study

From the above conclusions, there is need to further study the physical parameters of flocculation and the effects of change in the physical water-quality parameters on flocculation process. The objectives of this study are:-

1. To evaluate the effects of velocity gradient, G , and time of mixing, T , on flocculation process.
2. To optimize G and T for turbidity.
3. To optimize G and T for temperature.
4. To investigate the application of the results to design and operation of flocculators.

CHAPTER THREE

DESIGN OF EXPERIMENTAL INVESTIGATION

3.1 Scope of Study

Since coagulation-flocculation depends upon several independent variables, it was necessary to use an experimental method which provides control over as many parameters as possible while the effects of the chosen parameter(s) are studied. Synthetic kaolin suspension was used as the raw water sample because its treatment characteristics are in some ways similar to those of many river abstractions [21]. Laboratory scale batch reactors and aluminium sulphate coagulant were used in the study. Settled residual turbidity was used as the performance criteria with a desired performance level fixed.

3.2 Methodology

Literature Review

Literature from previous studies and other publications was reviewed with particular attention to the physical aspects of flocculation process.

Design of Mixing Equipment

The equipment was designed such that the value of the velocity gradient was controlled under each experimental conditions.

Sample and Reagents Preparation

Stock suspension/solutions of known strengths were prepared for ease of dilution to the required concentrations.

Experimental Study

The experimental procedure was derived from the conventional jar test procedure. A single factor method of optimization was used.

Analysis and Discussions of Results

Relationships between the various parameters under study were investigated. Discussions covered the experimental conditions, observations and the results; comparisons with previous findings in the literature were also done. Practical applications of results were also discussed.

3.3 Design of Mixing Equipment

The reactor and impeller geometry used is as shown in Figure 3.1. For this reactor-impeller geometry, Rafael and Letterman [28] developed a rating curve for water at 25°C as shown in Figure 3.3, curve "A".

Camp [7] developed rating curves for water at different temperatures; the reactor-impeller geometries and the rating curves are shown in Figure 3.4. From the curves for baffled reactor, it was found that for a given impeller speed the velocity gradient is proportional to the inverse square-root of dynamic viscosity. Using this relationship, curves "B", "C", and "D" in Figure 3.3 were projected from curve "A" for water temperatures of 10°C, 20°C, and 30°C, respectively, used in the study (section 3.5).

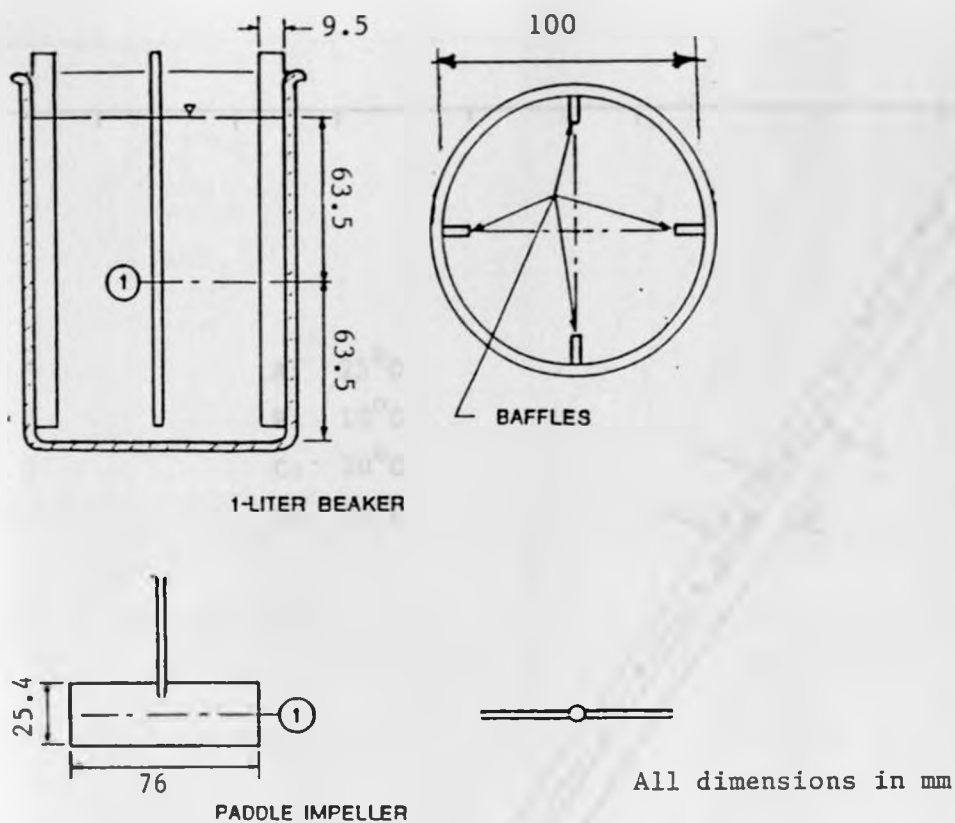


Fig.3.1 Reactor Geometry (Rafael and Letterman [28])

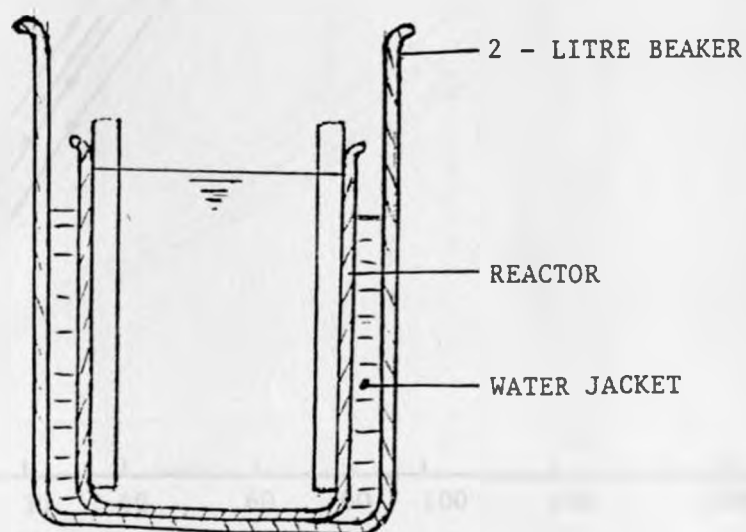


Fig.3.2 Reactor Arrangement

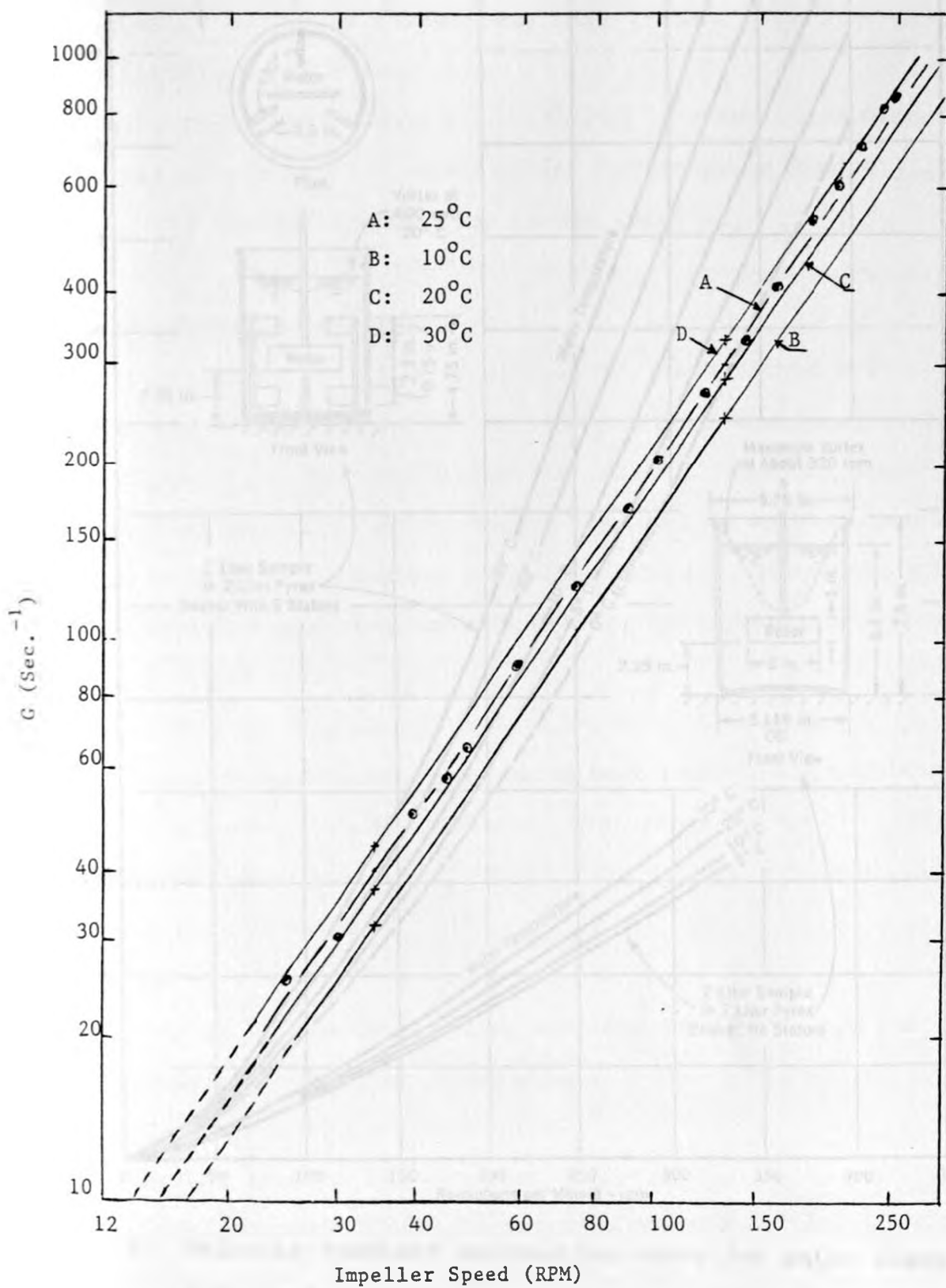


Fig.3.3 G versus impeller speed (modified from Rafael and Letterman [28]).

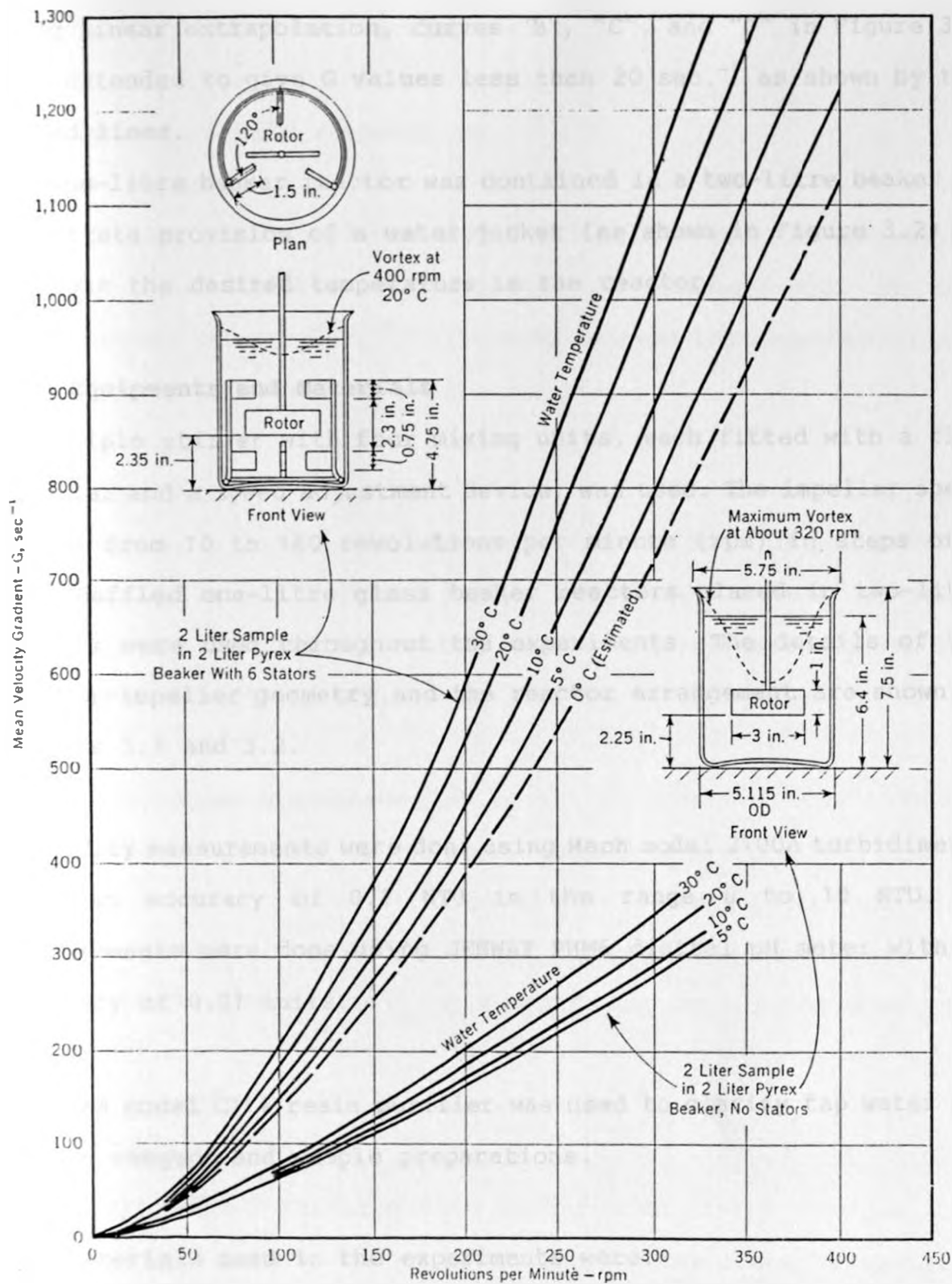


Fig.3.4. Velocity gradient calibration curve for water (Camp T.R. [7]).

Using linear extrapolation, curves "B", "C", and "D" in Figure 3.3 were extended to give G values less than 20 sec.^{-1} as shown by the dotted lines.

The one-litre beaker reactor was contained in a two-litre beaker to facilitate provision of a water jacket (as shown in Figure 3.2) to maintain the desired temperature in the reactor.

3.4 Equipments and Materials

A multiple stirrer with four mixing units, each fitted with a flat impeller and a speed adjustment device, was used. The impeller speed ranges from 10 to 160 revolutions per minute (rpm) in steps of 5 rpm. Baffled one-litre glass beaker reactors placed in two-litre beakers were used throughout the experiments. The details of the reactor-impeller geometry and the reactor arrangement are shown in Figures 3.1 and 3.2.

Turbidity measurements were done using Hach model 2100A turbidimeter with an accuracy of 0.1 NTU in the range 0 to 10 NTU. pH measurements were done using JENWAY PHM6 digital pH meter with an accuracy of 0.01 units.

ELGACAN model C114 resin purifier was used to clarify tap water for use in reagent and sample preparations.

The materials used in the experiments were:

- commercial grade aluminium sulphate crystal ($\text{Al}_2(\text{SO}_4)_3 \cdot 16 \text{H}_2\text{O}$).
- reagent grade sodium bicarbonate powder (99% W/W).
- analytical grade concentrated hydrochloric acid.

- Finely divided kaolin clay powder.

3.5 Reagents/Sample Preparation

Dilution Water

The "purified tap water" was used as dilution water. Three samples were kept at different temperatures i.e. around 4°C, at room temperature, and around 85°C. The samples were then blended to give the required temperature.

Alum Coagulant

The coagulant solution was prepared by dissolving 10 grams of the commercial alum in the dilution water to form one litre of solution; this solution was used without dilution [28]. Replacement was done after every five days [6].

Sodium Bicarbonate Solution

Reagent grade sodium bicarbonate powder was dissolved in the dilution water to a concentration of 10g/l. The solution was first gently stirred for 24 hours for it to gain equilibrium with the carbondioxide in the air; replacement was done after every two days [28].

Water sample

Water sample was prepared by mixing the finely divided clay particles in the dilution water to form a concentrated suspension. The suspension was first allowed to stand for one and a half hours in one-litre beaker; the supernatant was then used as the stock sample which was kept at room temperature. The turbidity of the

stock sample was determined to facilitate dilution to the required turbidity.

The upper limits of the physical quality parameters (temperature and turbidity) were adopted from the maximum average monthly values obtained from river Yamuna in India and river Nile in Sudan. These rivers are located in very hot regions and are prone to flooding due to incidence of high intensity rains and extensive agricultural activities in the immediate catchment.

The reported maximum average monthly turbidity for Yamuna river in India is 3300 NTU [17], four ranges of turbidity were identified for use in this study to represent low, medium, moderately high, and high turbidity; the respective ranges are: less than 60 NTU, 60 NTU to 200 NTU, 200 NTU to 800 NTU and greater than 800 NTU. The following turbidity values were used in the study to represent the respective range: 30 NTU, 120 NTU, 500 NTU, and 1200 NTU.

The maximum average monthly temperatures reported for river Nile in Sudan and river Yamuna in India was 36°C [17]; the following ranges were therefore considered in this study to represent low, medium, and high temperatures respectively: 4°C to 15°C, 15°C to 25°C, and 25°C to 36°C. The temperature values used in the study to represent the respective range were: 10°C, 20°C, and 30°C.

Alkalinity was added to the sample in form of sodium bicarbonate in an amount required to maintain the final pH at 7 ± 0.1 when the optimum dose of alum was used (section 3.6.3).

3.6 Experiments

3.6.1 General Principles

The experimental procedure was derived from the conventional jar test procedure. The following principles were applied in the study:

- Settled residual turbidity was used as the performance criteria. A level of 2.5 NTU was set to indicate the required performance (section 1.4.1) such that the optimum values of velocity gradient, G , and time of mixing, T , referred to those minimum values that gave the lowest residual turbidity in the neighbourhood of this set value.

A residential turbidity level of 2.5 NTU presents a very high level of treatment. This low level of residual turbidity was used because the contribution from excess metal hydroxides was removed by acidifying the sample to a pH of about 2.5 before turbidity measurement (see below).

- A single factor method of optimization as proposed by Cochram and Cox [11] was used.
- The supernatant was acidified to a pH of about 2.5 with concentrated hydrochloric acid before turbidity measurement. This procedure ensures greater reproducibility in turbidity measurements by dissolving the excess metal hydroxides in suspension hence reducing the effect of particle size in turbidity measurement [28].

3.6.2 Rapid Mix Process

Mhaishalkar et al [22] optimized G and T for rapid mix in treating kaolin suspension with alum; the results were shown in Table 2.1 (section 2.2).

The multiple stirrer used had a maximum speed of 160 r.p.m. (section 3.4) corresponding to a velocity gradient of $350s^{-1}$ for water at $10^{\circ}C$ (Figure 3.3). This velocity gradient and retention time of 100 seconds were used to give the product GT value of 35,000 which is the average of the values in Table 2.1 (Section 2.2). This rapid mix condition was used throughout the experiments.

3.6.3 Preliminary Experiments

Preliminary experiments were conducted to: determine the optimum coagulant dosages; determine the alkalinity level required for pH adjustments; and evaluate temperature control.

Optimum Coagulant Dose

Optimum coagulant dose was determined for each turbidity value under study. It was desired that for each turbidity value, a fixed amount of coagulant be used irrespective of temperature. Since more coagulant is required at lower temperatures [6], the optimum dose for a given turbidity was determined at $10^{\circ}C$ (section 3.5) and this dose was used for all other temperatures.

The procedure followed in optimizing coagulant dose was as follows:-

- (i) One litre samples at $10^{\circ}C$ and of a given turbidity were measured off in four reactors; the reactors were then positioned under the impellers.

- (ii) An amount of sodium bicarbonate (in mg/l) corresponding to one-half the turbidity value was added in each reactor to provide alkalinity.
 - (iii) The impellers were turned on at a velocity gradient of 350 sec^{-1} (section 3.6.2) and using syringes, measured volumes of alum solution were rapidly injected into the reactors and the stop clocks immediately started.
 - (iv) After 100 seconds of rapid mixing (section 3.6.2), the velocity gradient was reduced to 50 sec^{-1} and gentle mixing continued for 20 minutes.
- Note: Velocity gradient of 50 sec^{-1} was found to be applicable to a wide range of flocculation processes [19].
- (v) Immediately after gentle mixing, the reactors were removed from the stirrers and the suspension allowed to settle under quiescent condition for 25 minutes.
 - (vi) After settling, about 80 ml sample of the supernatant was siphoned into a flask from about 5 cm below the surface.
 - (vii) Two drops of conc. hydrochloric acid were added to the sample and the sample vigorously shaken before turbidity measurement (section 3.6.1).
 - (viii) The optimum coagulant dose was got from a plot of residual turbidity versus coagulant dose.

pH Adjustment

The final pH was to be maintained at 7 ± 0.1 throughout the experiments and this was achieved by adding sufficient alkalinity in form of sodium bicarbonate to buffer the coagulant reactions; optimum pH range for alum is 6.5 to 7.5 [6].

The procedure for determining the required sodium bicarbonate dose was as follows:-

- (i) One-litre samples of a given turbidity at room temperature were measured off in four reactors.
- (ii) Different dosages of sodium bicarbonate were added to the reactors and the reactors positioned under the impellers.
- (iii) The impellers were turned on at a velocity gradient of about 350 sec.^{-1} and the optimum coagulant dose as determined above was added using syringes.
- (iv) Rapid mixing continued for 100 seconds then gentle mixing at velocity gradient of 50 sec.^{-1} followed for 20 minutes.
- (v) After mixing, the pH was determined and a plot of pH versus bicarbonate dose gave the required dose for a final pH of 7.

Evaluation of Temperature Changes

The dilution water was first blended to give the test temperature (section 3.5). Room temperature varied from 19°C to 24.5°C during the experiments. Temperature variations in the reactors were countered by the introduction of cold or hot water jacket depending on the situation; a variation of $\pm 1.0^{\circ}\text{C}$ about the test value was acceptable.

For the 10°C sample, the temperature was first set at about 9.5°C . When the temperature rose to about 10.5°C , a water jacket at about 4°C and 95mm deep (fig. 3.1 and 3.2) would be introduced; the temperature would drop to about 10.3°C . When the temperature reached 10.5°C again and mixing was to continue; the spent water jacket would be siphoned out and then replaced.

For the 20°C sample, water jacket was not used as the test temperature was near the room temperature. Temperature variation was within $\pm 0.5^{\circ}\text{C}$.

For the 30°C sample, the temperature was first set at 30.5°C. When the temperature dropped to about 29.5°C, a water jacket at about 90°C and 40mm deep would be introduced; the temperature would rise to about 30.5°C. More hot water would be added in the water jacket when required.

In all cases no controls were provided during settling except for the 30°C samples where reactors were covered with aluminium foil to reduce thermal eddies in the reactors.

3.6.4 Final Experiments - Optimization

Rapid mix conditions, settling, and turbidity measurements were as described in section 3.6.3.

The procedure for the single factor method of optimization used in the experiments was as given below.

For a given temperature and turbidity, the flocculation velocity gradient, G , and the mixing time, T , were optimized as follows:-

- (i) A mixing time, T , was selected and fixed.
- (ii) A series of tests were run with different values of G for mixing time in (i) above.

- (iii) Optimum G , G_{opt} , was obtained from a plot of residual turbidity versus G ; a minimum G value which gave a residual turbidity of about 2.5 NTU (section 3.6.1) was taken as G_{opt} .
- (iv) Fixing velocity gradient at G_{opt} in (iii) above, a series of tests were run for various mixing times.
- (v) Optimum T , T_{opt} , was obtained from a plot of residual turbidity versus T ; T_{opt} was the minimum mixing time that gave a residual turbidity of about 2.5 NTU.
- (vi) If T_{opt} in (v) above was found to be close to T in (i) above then G_{opt} and T_{opt} obtained were the actual optima for the given temperature and turbidity. But if there was a big difference between T and T_{opt} then steps (i) through (v) would be repeated starting with T_{opt} in (v) as a better approximation.

	25	35	45
	40	70	100
	120	180	240
	300	600	900

CHAPTER FOUR

RESULTS, ANALYSIS AND DISCUSSIONS OF RESULTS

4.1 Experimental Data

Preliminary Experiments

The data from the preliminary experiments are shown in table A2-1 and A2-2 and the respective figures A2-1 and A2-2 (Appendix 2). The summary of results is presented in table 4.1 below.

Table 4.1 Preliminary Experiments Results

Turbidity (NTU)	Alum Dose (mg/l)	Na HCO ₃ Dose (mg/l)	Final pH
30	20	45	6.96
120	30	70	7.03
500	120	300	7.03
1200	275	600	7.0

Final Experiments - Optimization

The data from the optimization experiments are shown in tables A1-1 to A1-4 (Appendix 1) and plotted in figures 4.1 to 4.4 below.

For a given experimental condition, the velocity gradient, G , and the time of mixing, T , were minimized alternately to give a residual turbidity of 2.5 NTU as the desired performance (section 3.6.4);

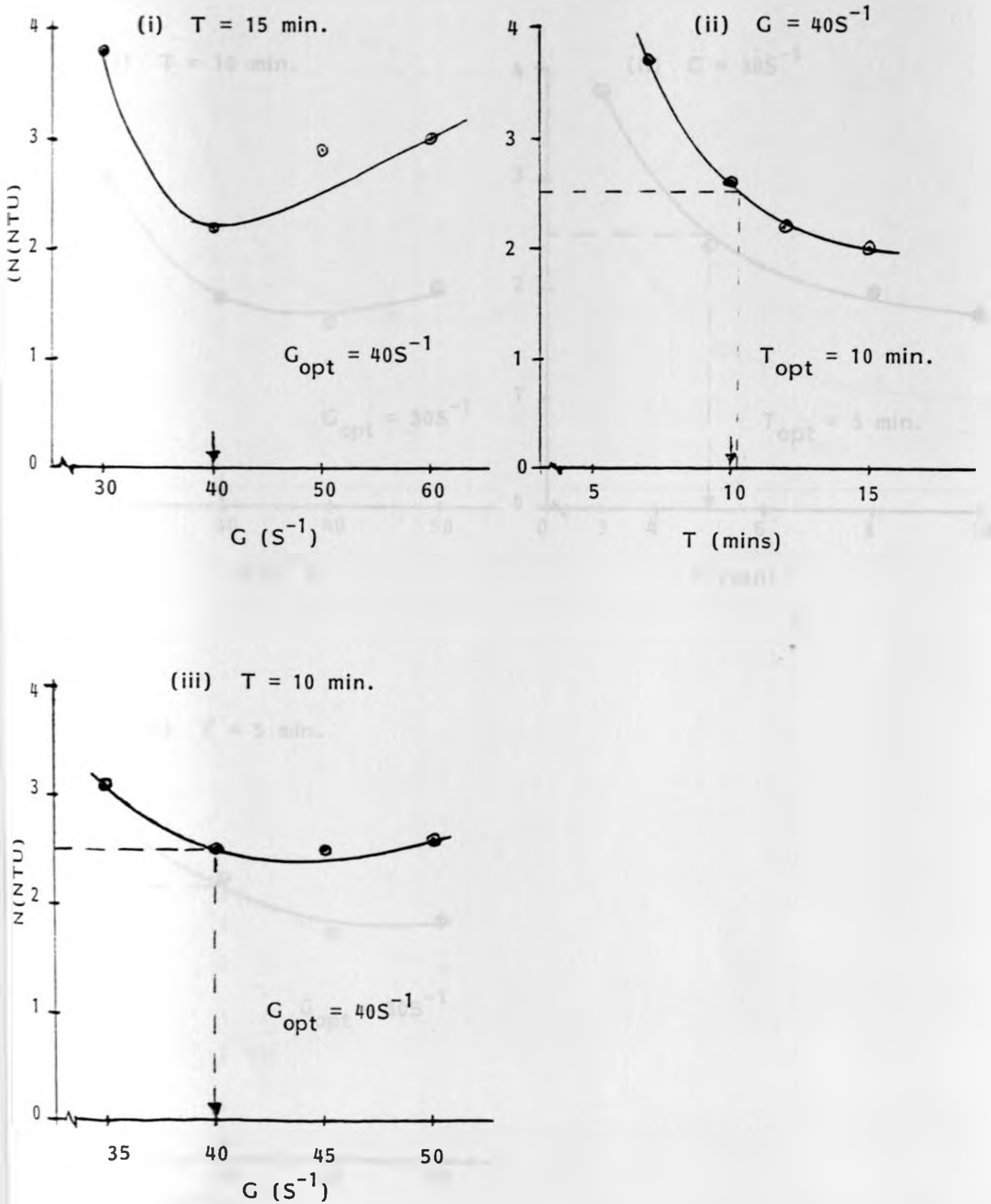


Fig. 4.1 a. Optimal G and T for raw water turbidity of 30 NTU and temperature of 10°C .

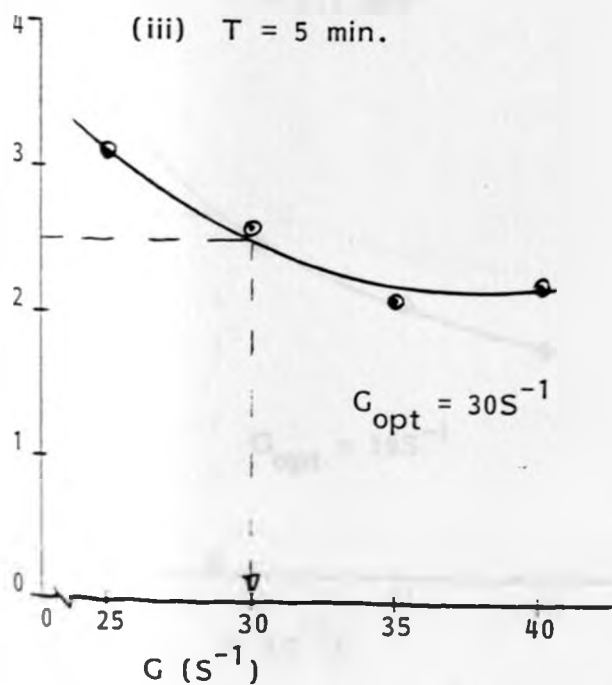
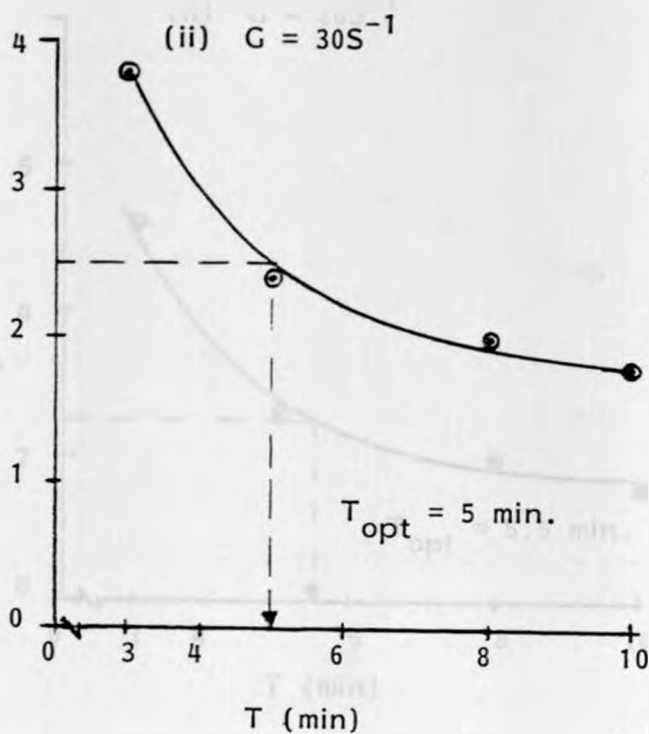
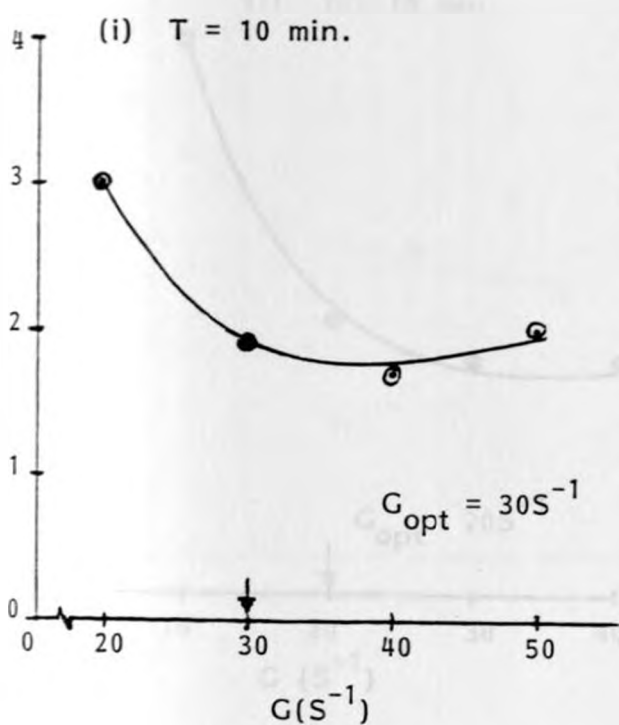


Fig. 4-1b. Optimal G and T for raw water turbidity of 30 NTU and temperature of 20°C .

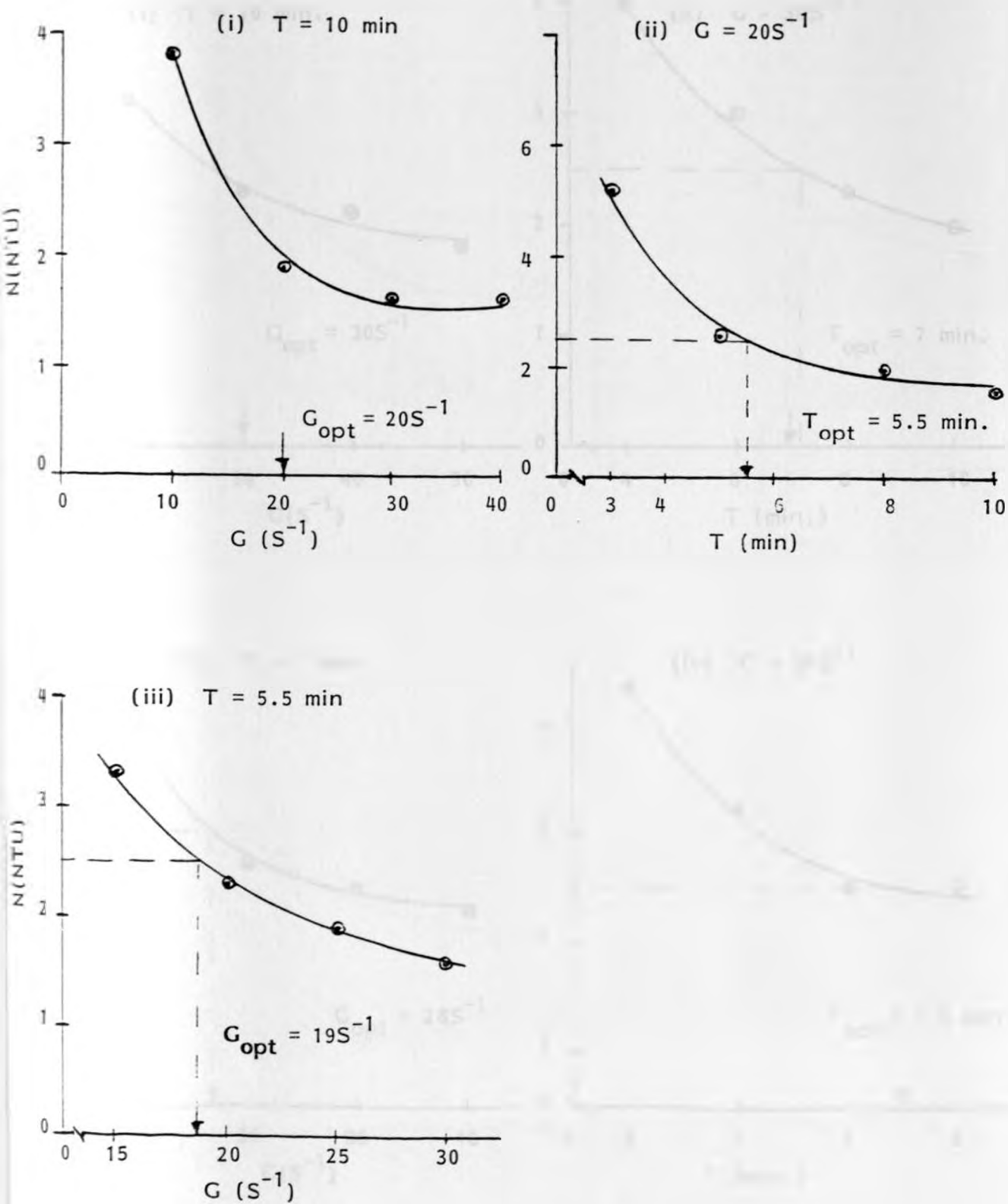


Fig. 4.1 c. Optimal G and T for raw water turbidity of 30 NTU and temperature of 30°C .

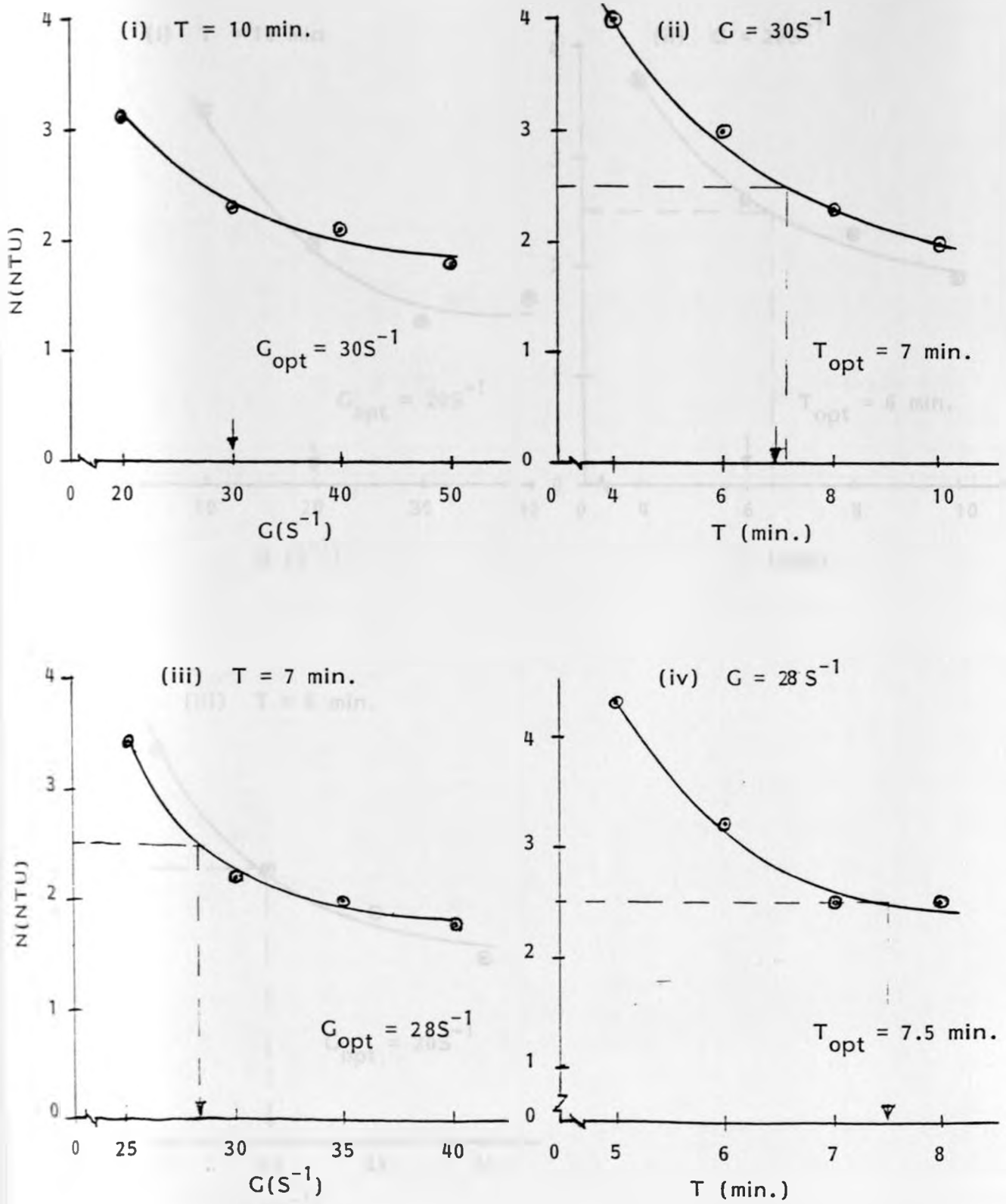


Fig. 4.2 a. Optimal G and T for raw water turbidity of 120 NTU and temperature of 10°C.

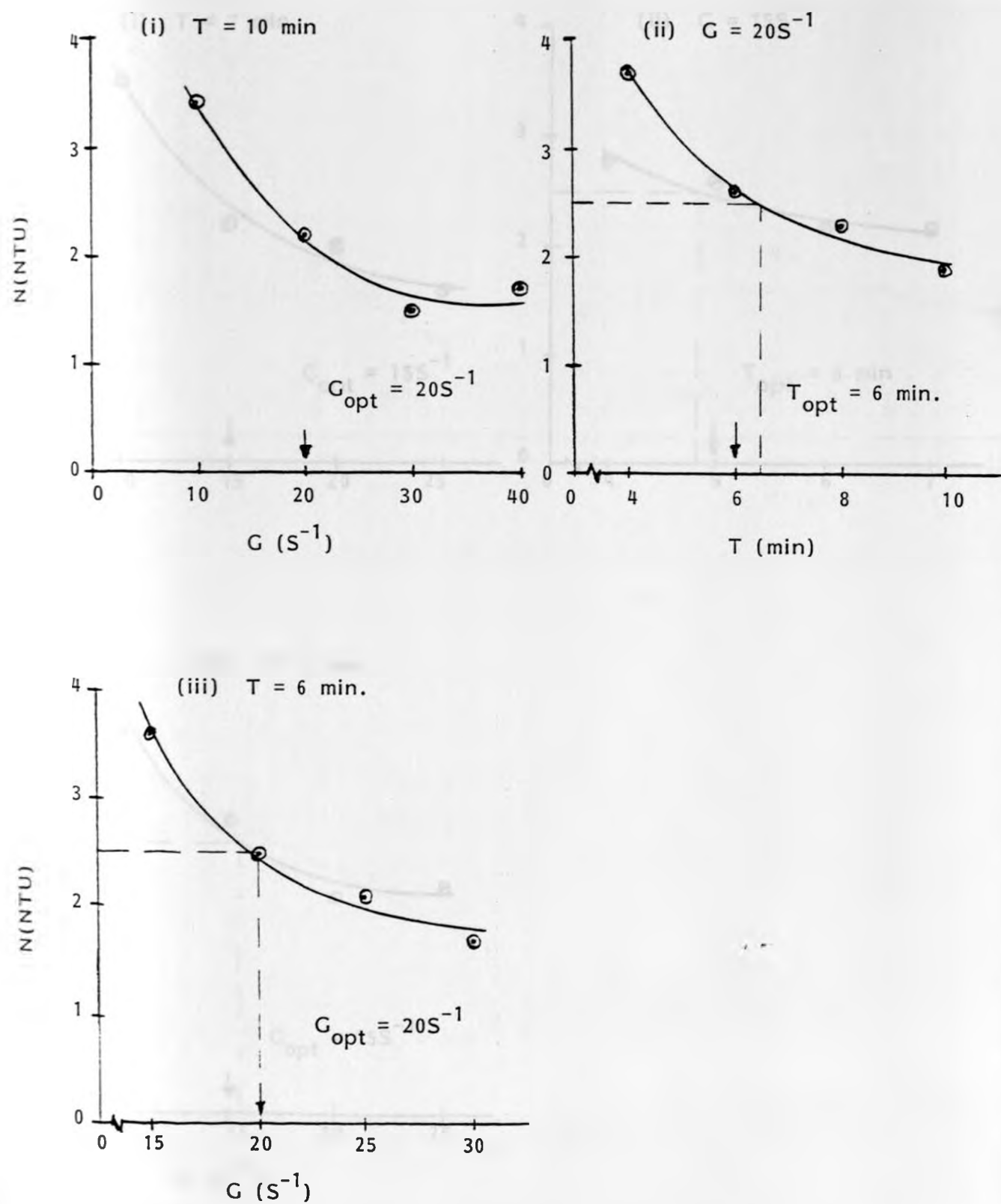


Fig. 4.2 b. Optimal G and T for raw water turbidity of 120 NTU and temperature of 20°C .

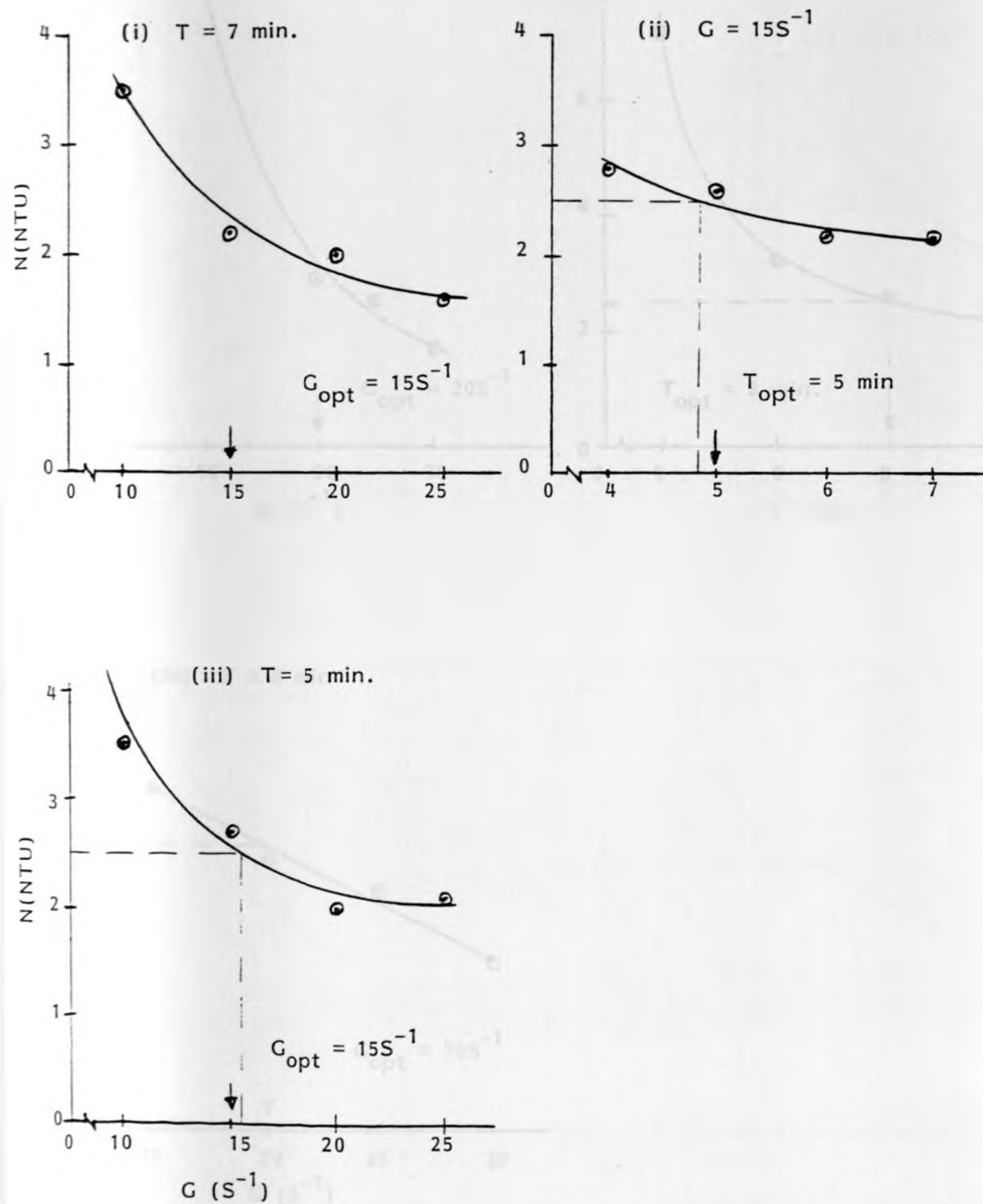


Fig. 4.2 c. Optimal G and T for raw water turbidity of 120 NTU and temperature of 30°C .

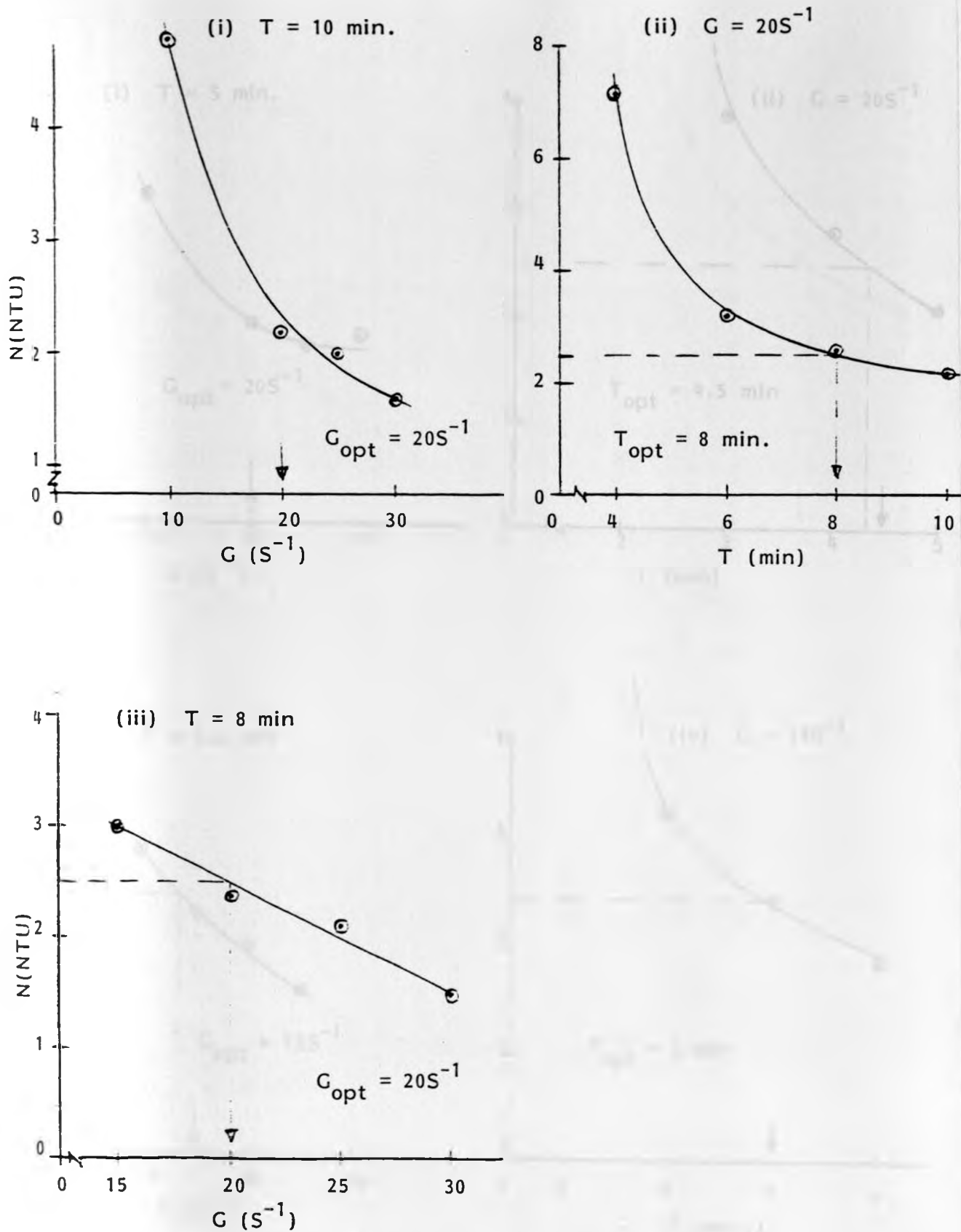


Fig. 4.3 a. Optimal G and T for raw water turbidity of 500 NTU and temperature of 10°C .

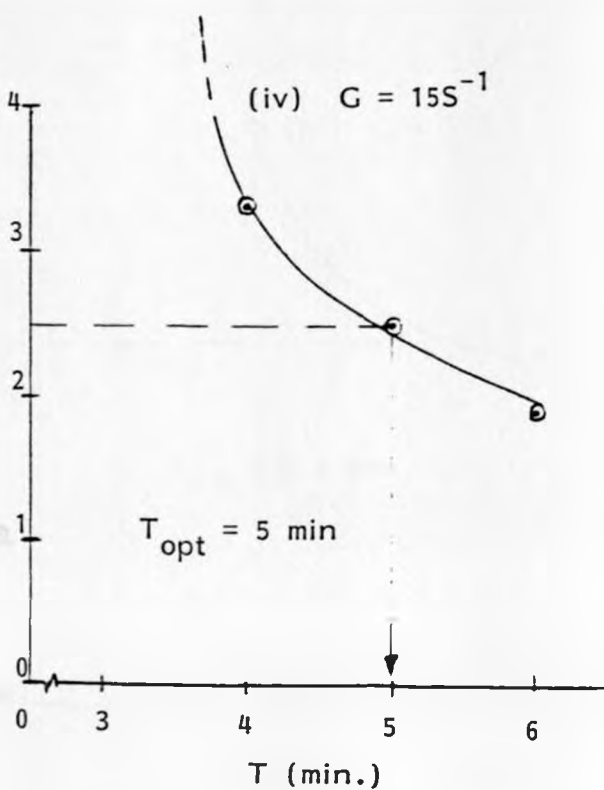
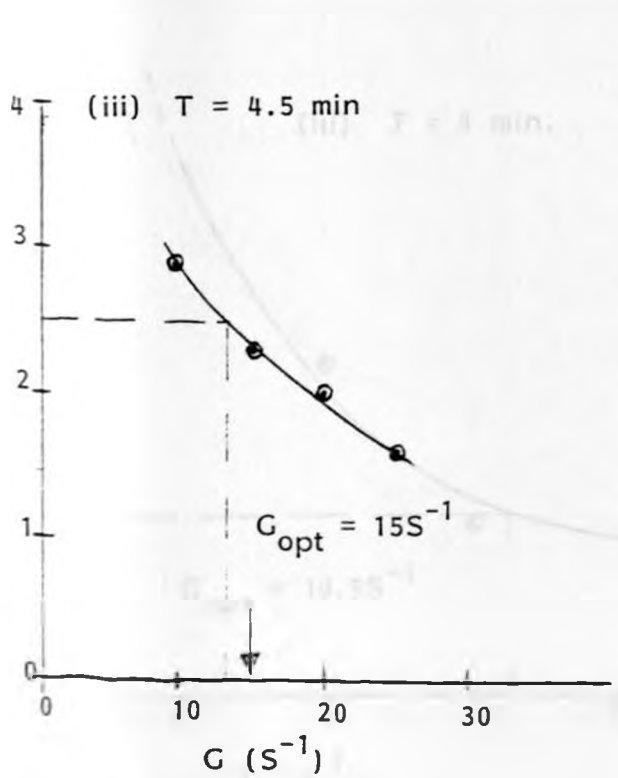
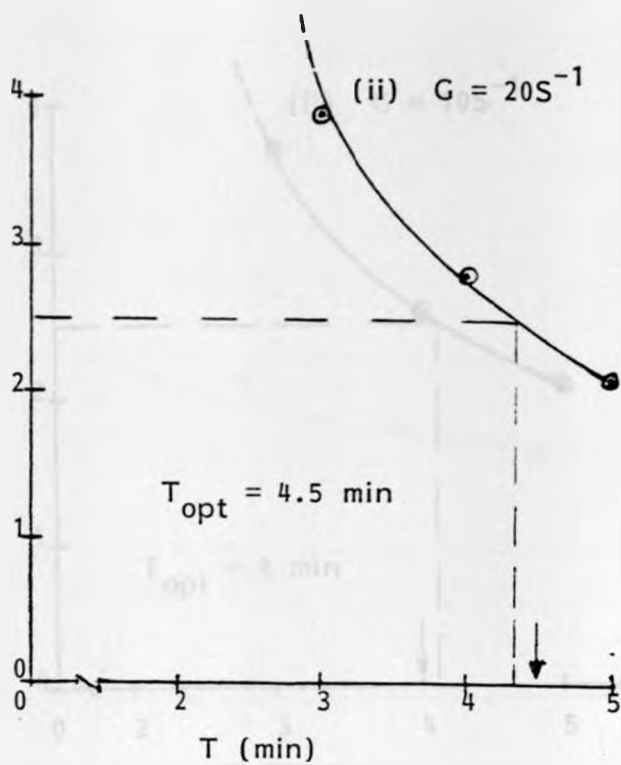
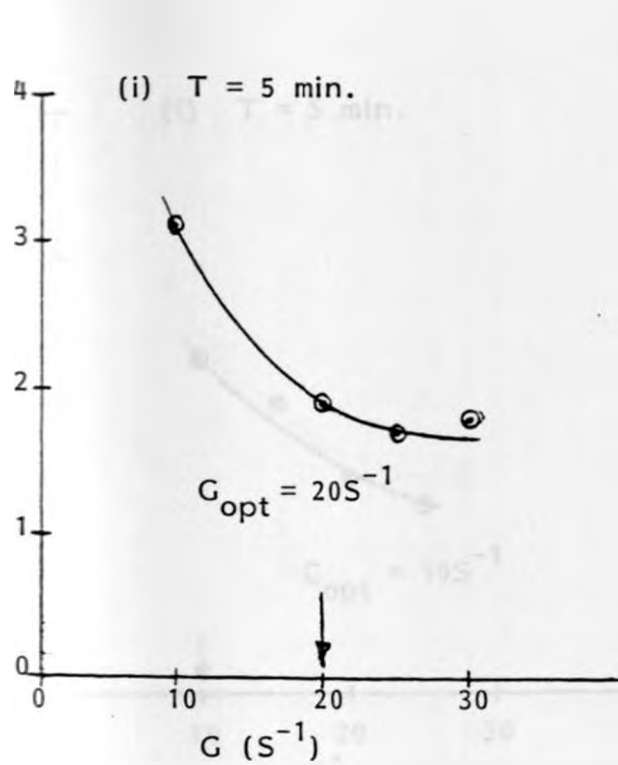


Fig. 4.3 b. Optimal G and T for raw water turbidity of 500 NTU and temperature of 20°C .

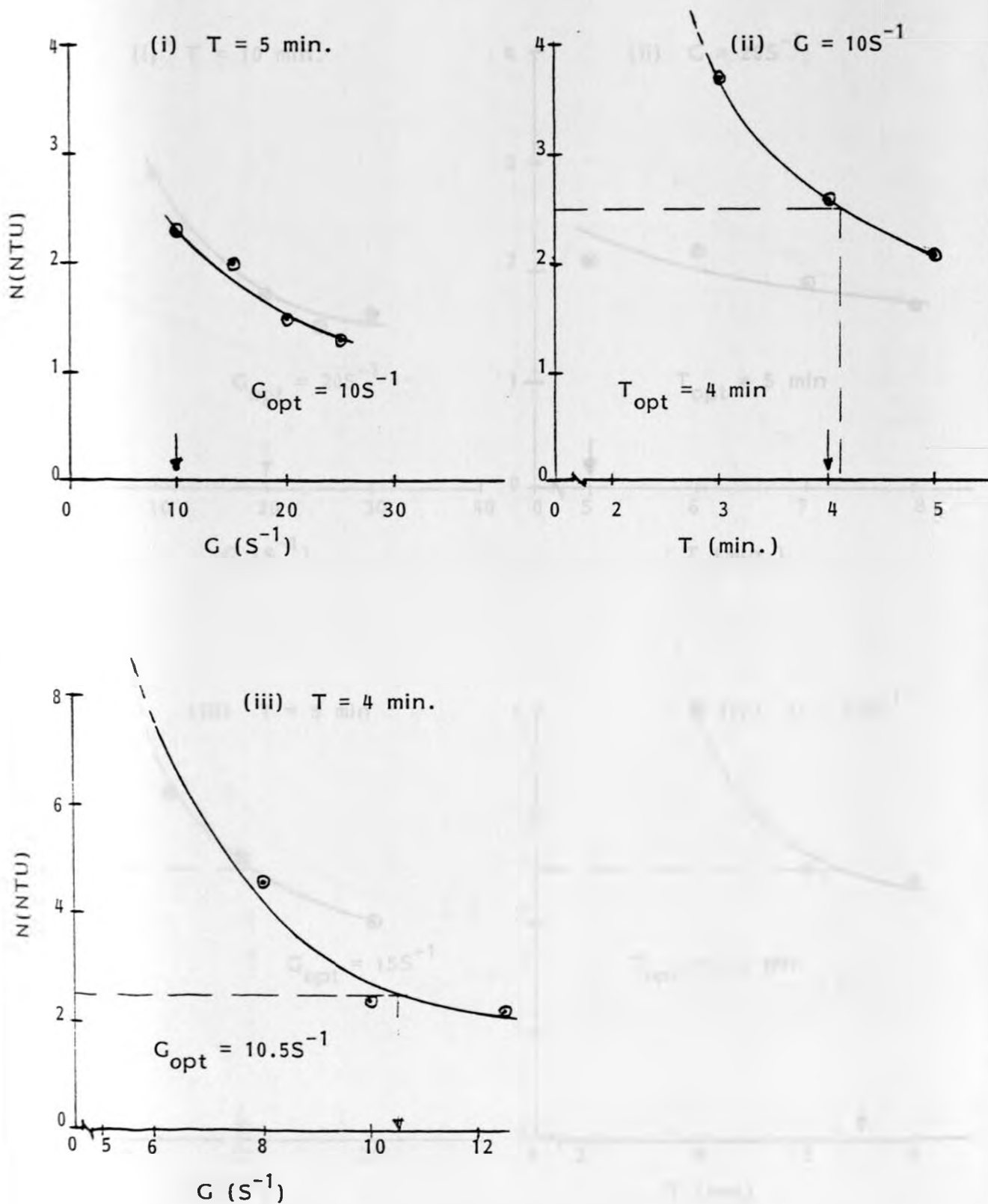


Fig. 4.3 c. Optimal G and T for raw water turbidity of 500 NTU and temperature of 30°C .

N(NTU)

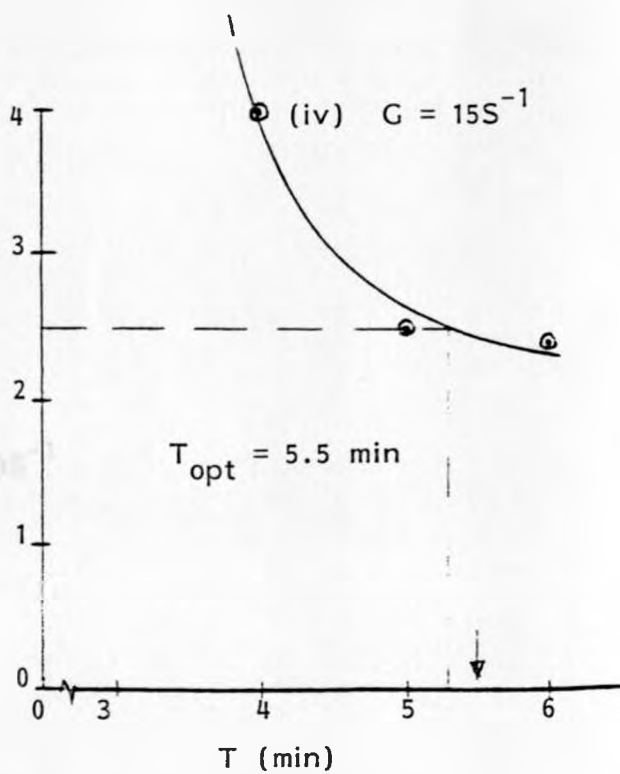
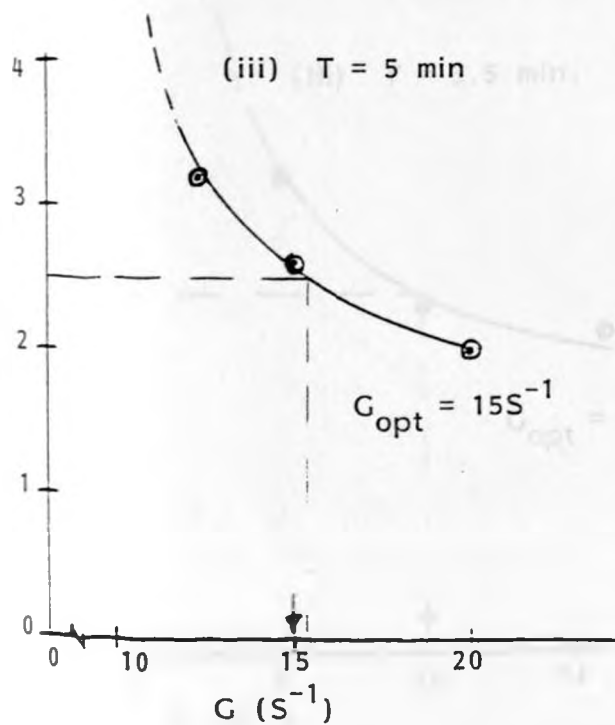
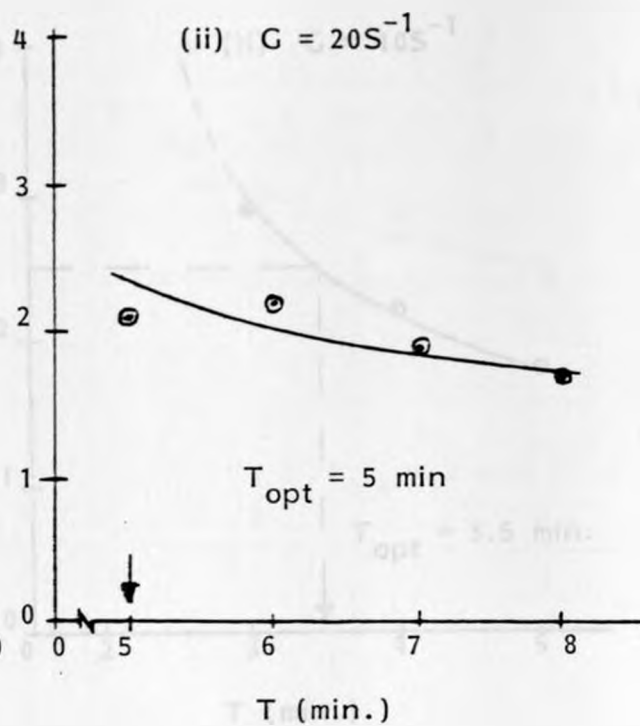
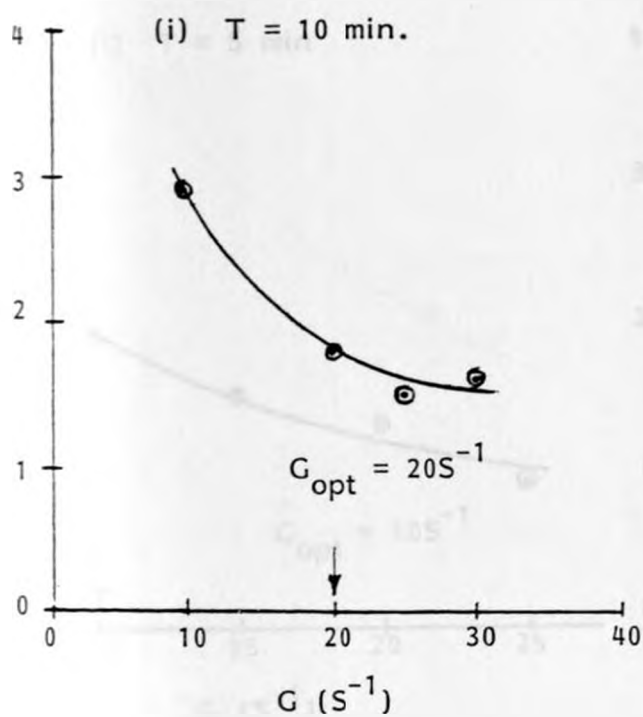


Fig. 4.4 a. Optimal G and T for raw water turbidity of 1200 NTU and temperature of 10°C .

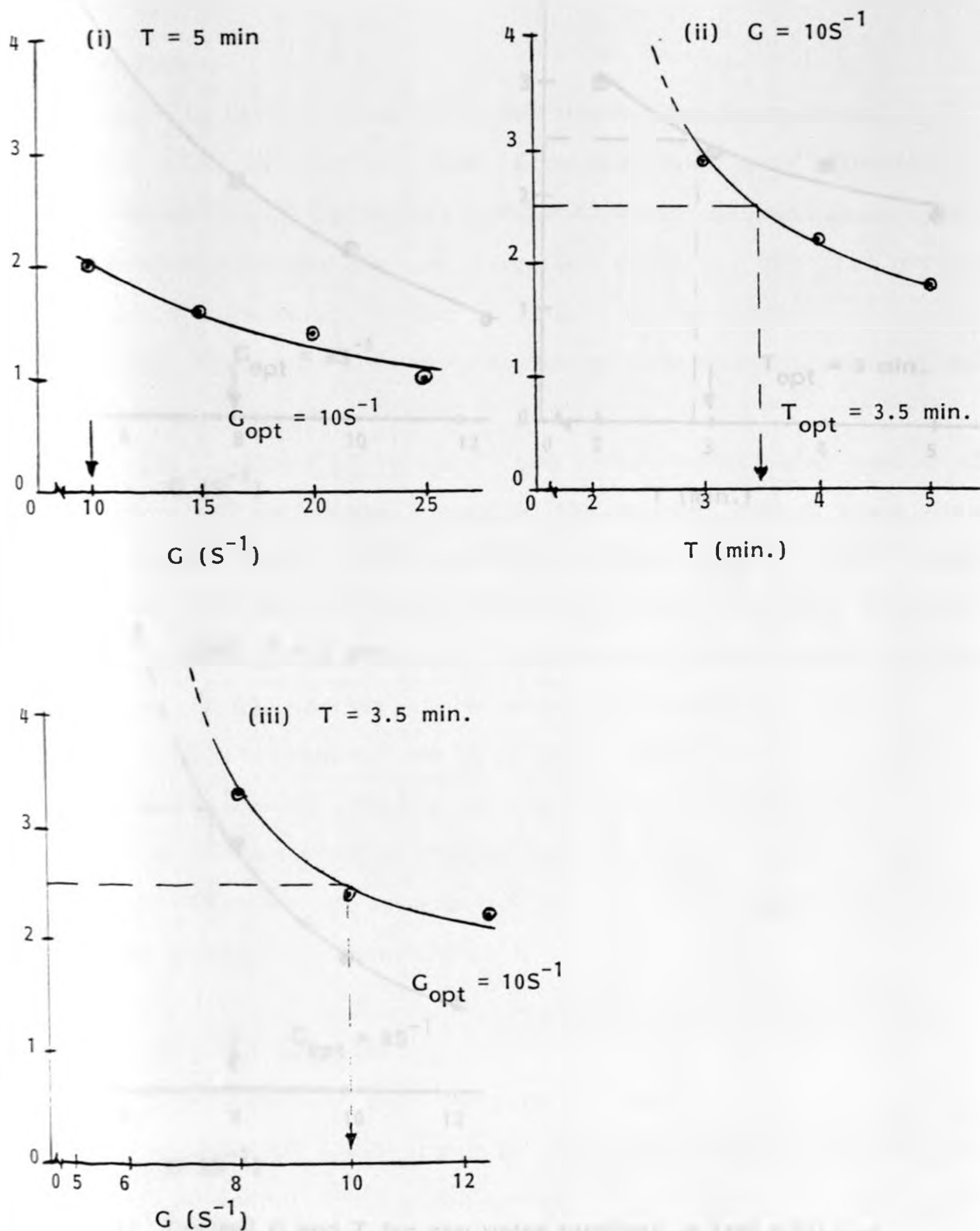


Fig. 4.4 b. Optimal G and T for raw water turbidity of 1200 NTU and temperature of 20°C .

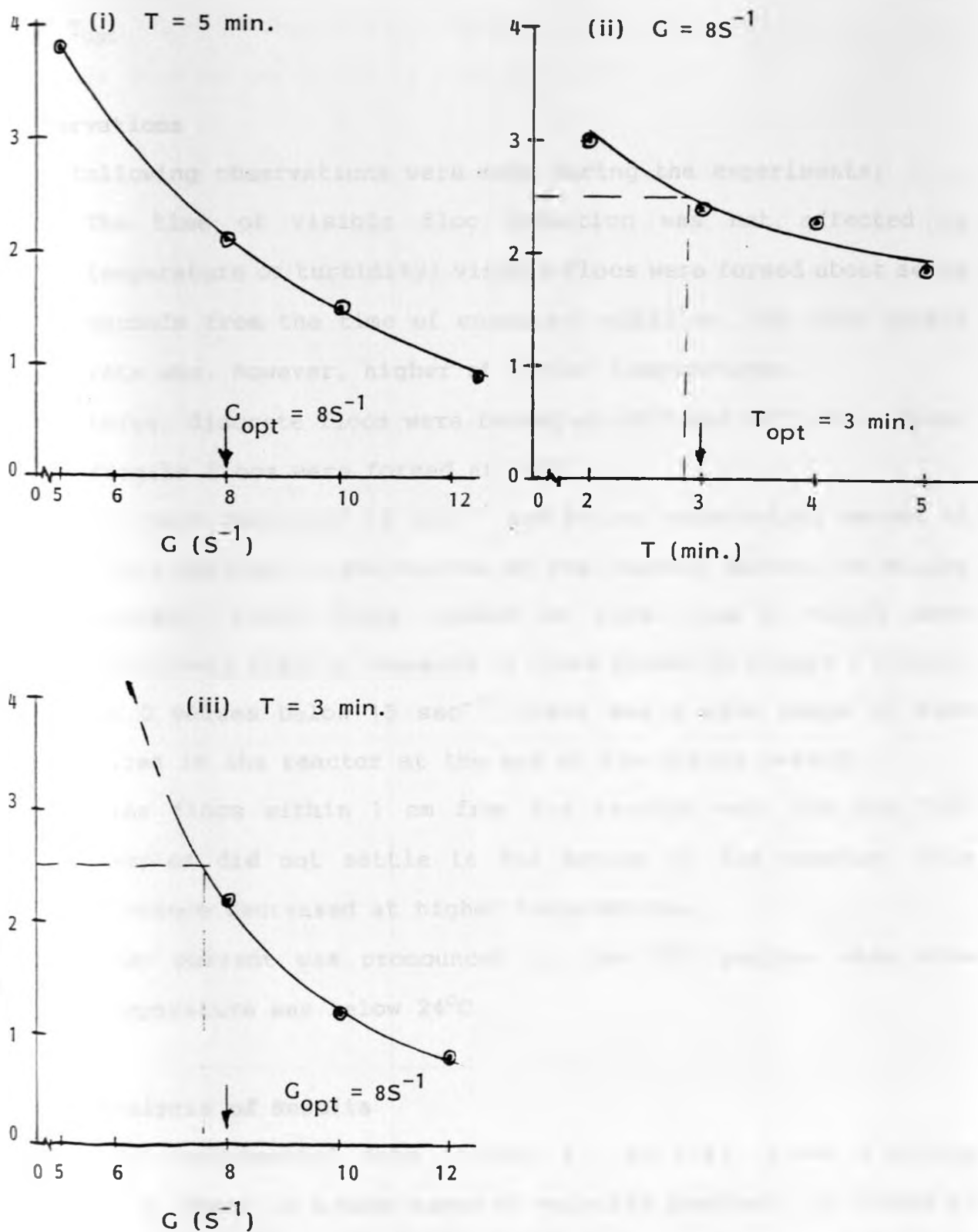


Fig. 4.4 c. Optimal G and T for raw water turbidity of 1200 NTU and temperature of 30°C .

these minimum values of G and T were the corresponding optima, G_{opt} and T_{opt}

Observations

The following observations were made during the experiments:

- The time of visible floc formation was not affected by temperature or turbidity; visible flocs were formed about seven seconds from the time of coagulant addition. The floc growth rate was, however, higher at higher temperatures.
- Large, discrete flocs were formed at 20°C and 30°C while fine, fragile flocs were formed at 10°C.
- At low G values of 10 sec^{-1} and below, substantial amount of flocs settled to the bottom of the reactor during the mixing process. Also, flocs formed at these low G values were relatively fragile compared to those formed at higher G values.
- At G values below 15 sec^{-1} , there was a wide range of floc sizes in the reactor at the end of the mixing period.
- Fine flocs within 1 cm from the reactor wall for the 10°C samples did not settle to the bottom of the reactor; this distance decreased at higher temperatures.
- Eddy current was pronounced in the 30°C samples when room temperature was below 24°C.

4.2 Analysis of Results

From the experimental data (figure 4.1 to 4.4), given a mixing period, T , there is a wide range of velocity gradient, in excess of the optimum value, that gives better performance; this was also pointed out by Argaman and Kaufman [4] (section 2.2). Also,

extended mixing at an optimum G values gives improved performances; this was also demonstrated by Rafael and letterman [28] (fig. 2.2) for the case of low velocity gradient of 25 sec.⁻¹.

The results of the optimization experiments are summarized in table 4.2 below. The optima, G_{opt} and T_{opt} were obtained from the last two runs in each set of experiment (i.e. for a given temperature and turbidity).

Table 4.2 Summary of Final Experiments Results

Turbidity No(NTU)	Temperature t(°C)	$G_{opt}(\text{sec.}^{-1})$	$T_{opt}(\text{min.})$	$G_{opt}^* \cdot T_{opt}$
30	10	40	10	24,000
	20	30	5	9,000
	30	19	5.5	6,270
120	10	28	7.5	12,600
	20	20	6	7,200
	30	15	5	4,500
500	10	20	8	9,600
	20	15	5	4,500
	30	10.5	4	2,520
1200	10	15	5.5	4,950
	20	10	3.5	2,100
	30	8	3	1,440

The relationships between the various parameters (4.2) are shown in Figures 4.5, 4.6, and 4.7.

Fig. 4.5 shows a linear relationship between the optimum velocity gradient, G_{opt} and the logarithm of the raw water turbidity at a given temperature. The optimum G for a given turbidity is higher at lower temperature; meanwhile for a given temperature, optimum G is higher at lower turbidity. Also, the difference between the optimum G values at different temperatures is higher at lower turbidities than at higher turbidities signifying that the effects of temperature on flocculation process is more pronounced at lower turbidity values. For a given water source, optimum G can be obtained from such graphs when the raw water turbidity and temperature are known.

Fig. 4.6 shows a linear relationship between the dimensionless product, $G_{opt} \cdot T_{opt}$, and the logarithm of the raw water turbidity at a given temperature; the higher the turbidity and/or temperature, the lower the power requirement. Also from Fig. 4.6, the drop in power requirements with increase in turbidity is much higher at 10°C than at 20°C and 30°C ; by extrapolating these graphs, it is apparent that at a raw water turbidity of about 4,000 NTU, no power input is required for flocculation at all temperatures.

Fig. 4.7 shows a linear relationship between the logarithm of the optimum velocity gradient and the logarithm of the optimum mixing time at all temperatures and turbidities; the higher the optimum G value the higher the optimum T . Therefore for a given source of

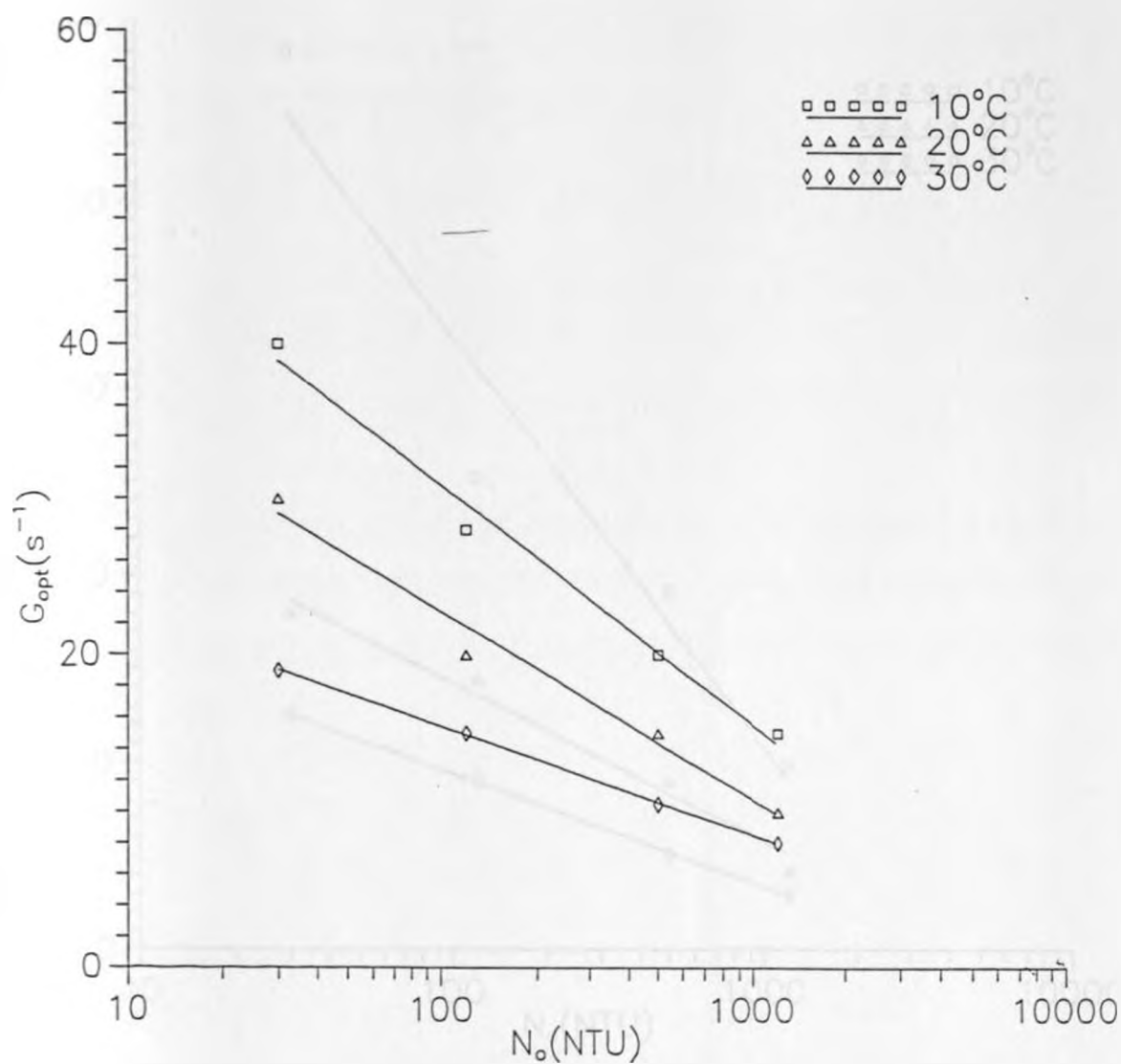


Fig.4.5. G_{opt} as a Function of Raw Water Turbidity.

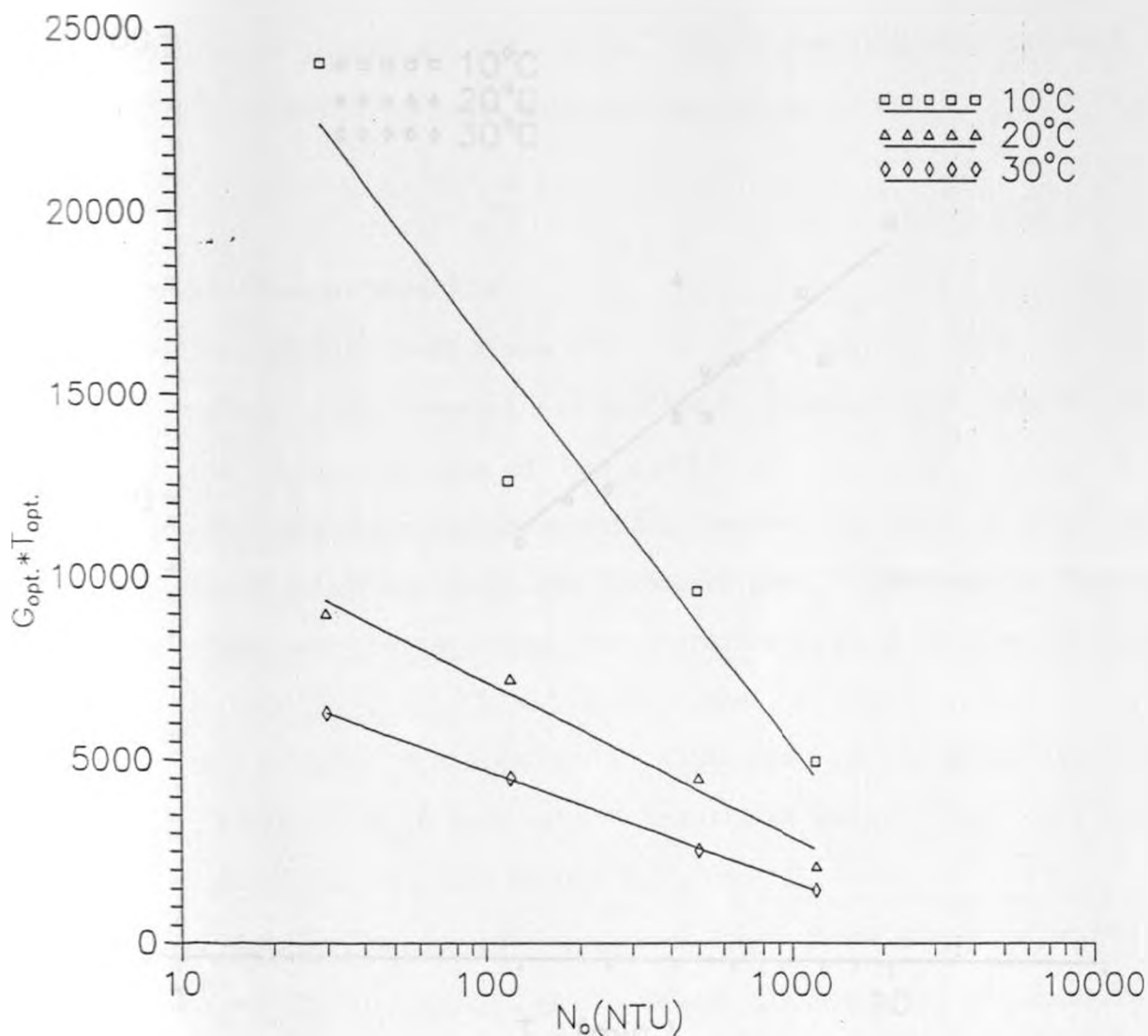
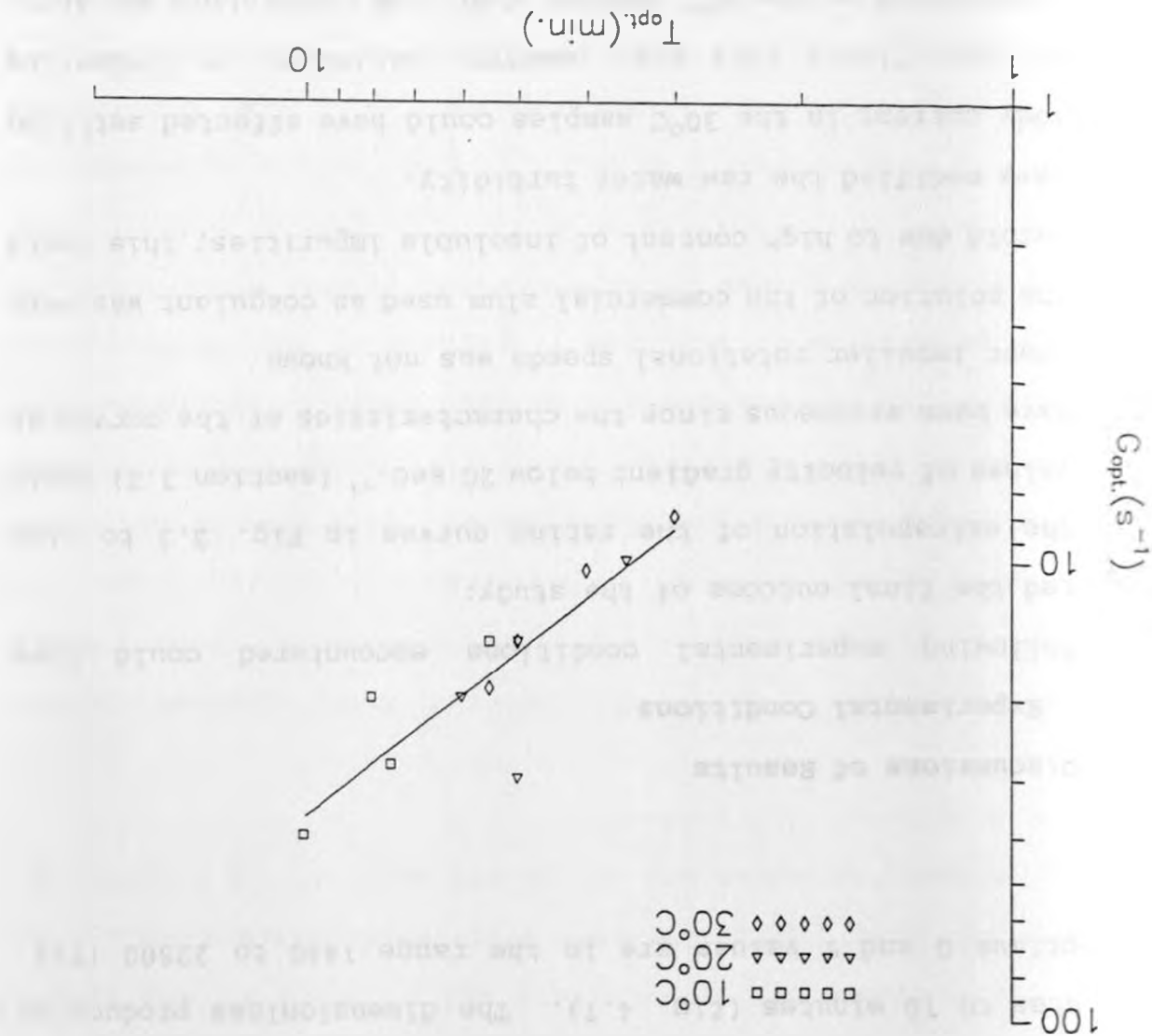


Fig.4.6. $G_{opt.} * T_{opt.}$ as a Function of Raw Water Turbidity.

Fig.4.7. G_{opt} as a Function of T_{opt} .

water, only one such graph is used to determine optimum T after optimum G is determined from fig. 4.5.

The optimum velocity gradient obtained are in the range 8 sec.^{-1} to 38 sec.^{-1} (fig. 4.5) while the optimum mixing time are in the range 3 minutes to 10 minutes (fig. 4.7). The dimensionless product of the optimum G and T values are in the range 1440 to 22500 (fig. 4.6).

4.3 Discussions of Results

4.3.1 Experimental Conditions

The following experimental conditions encountered could have affected the final outcome of the study:

- The extrapolation of the rating curves in Fig. 3.3 to give values of velocity gradient below 20 sec.^{-1} (section 3.3) could have been erroneous since the characteristics of the curves at lower impeller rotational speeds was not known.
- The solution of the commercial alum used as coagulant was very turbid due to high content of insoluble impurities; this could have modified the raw water turbidity.
- Eddy current in the 30°C samples could have affected settling of fine flocs; this was, however, minimized by conducting experiments on the 30°C samples when room temperature was above 24°C (section 4.1.2.).
- Water temperatures varied in the ranges $10 \pm 1^{\circ}\text{C}$, $20 \pm 0.5^{\circ}\text{C}$, and $30 \pm 0.5^{\circ}\text{C}$; the higher variations for the 10°C samples could have had more effects on the performance.

4.3.2 Results

The findings that for a given T there is a wide range of G in excess of G_{opt} that give better performance and that extended mixing at G_{opt} gives improved performance (section 4.2) indicates that an optimum design for a given temperature or turbidity can perform better at some higher temperature or turbidity values since in the latter cases optimum power inputs are lower (fig. 4.6). Hence a small rise in physical quality parameters of the raw water should not warrant a change in flocculation parameters.

The optimum G and T values obtained are small compared to the recommended values used in practice. American Water Works Association [33] recommended G in the range 5 to 100 sec.^{-1} and T in the range 20 to 60 minutes while minimum T value usually quoted is 10 minutes; required to minimize after-floc formation [19, 10]. The magnitude of the optimum G and T in this case, where the desired level of performance is set, are a function of the sedimentation period used; higher values are expected when shorter settling period is used. This is in contrast with the findings of Griffith and William [16] that optimum G is not a function of the sedimentation period; they did not set the performance level. Also the optimum G and T in this study are the minimum values of both G and T to give the desired performance.

The relationship that the higher the optimum G value the higher the optimum T (fig. 4.7) is in contrast with the findings of Argaman and Kaufman [4] (fig. 2.3) that the longer the mixing time the lower the optimum G ; this is due to the differences in experimental

conditions: the optimum G used by the authors [4] was the G value that maximized turbidity removal given an arbitrary retention time, T and the level of performance was not of importance but in this study, the optimum values of G and T used were those minimum values that would give a desired performance. The combination of low optimum G with low optimum T signifies a much lower power input at higher temperatures and/or turbidities; this is illustrated in Fig. 4.6 where the power function, $G.T.$, is plotted against turbidity.

The decrease in power requirement with increasing turbidity is because the collision chances at higher turbidity are higher due to increased solids concentration. Also at high turbidities, mixing due to differential settling of solids becomes more significant upto the point when external mixing is not necessary i.e. in this case, when turbidity is greater than 4,000 NTU; due to low velocity gradient induced under this condition, low density flocs are formed.

The high power requirement at low temperatures can be attributed to four factors:

- the shear resistance is higher at low temperatures due to high viscosity and this requires high shear stresses to be set up for achievement of proper mixing.
- due to high viscosity at low temperatures, the laminar sublayers that develop on the walls and blades are thicker than at high temperatures [13, 29] and this requires high energy input to overcome fluid friction that develops in the sublayer. Also because of this thick sublayer, there is poor velocity gradient distribution in the reactor and thus inefficient power

utilization; laminar sublayer is suppressed by high turbulence [29].

- the efficiency of the rapid mix process is lower at low temperatures since mixing by Brownian diffusion plays a big role in the formation of microflocs [6]; high viscosity is therefore a hindrance to this process.
- the poor settling condition under high viscosity requires flocs of good settleability i.e. high density flocs which are produced under high velocity gradient [7].

The formation of fragile flocs at low velocity gradients is a result of low collision energy between particles. At these low velocity gradients the flow regime in the reactor is predominantly laminar and thus collision is mainly due to relative velocities between streamlines. In the case of fragile flocs formed at low temperatures, the effect of high viscosity could also come in i.e. although velocity gradients are relatively high in this case, particles diffusion out of the streamlines is hampered by the high viscosity thus collision is mainly due to relative velocities between streamlines.

4.3.3 Practical Applications of Results

The direct application of these results in design and operation of flocculators is not recommended; project-designed experimental procedure should be used on the water to be treated and should address factors like the raw water quality, the desired performance, and the sedimentation period in the full scale plant.

The knowledge of variations in the optimum flocculation parameters with respect to the physical parameters of raw water is important in the design of a flexible flocculation system to ensure optimum operation. In hydraulic mixers where flexibility in operation is limited, optimum operation can be maintained by modifying the raw water quality to match the design conditions; this modification involves addition of turbidity to the raw water when natural turbidity and/or temperatures are low. Generally addition of turbidity to water of low turbidity (and temperature) is an attractive alternative to reduce costs of water treatment by flocculation; the worst flocculator design condition is when the raw water turbidity and temperature are low.

CHAPTER FIVE

CONCLUSIONS AND RECOMMENDATIONS

5.1 Conclusions

The suspended solids concentration was identified as the decisive control parameter in flocculation. The optimum mixing condition depends on raw water turbidity and temperature, treatment level, and sedimentation period. The relationships between the various physical parameters of flocculation and raw water quality were investigated in this study and the following conclusions were made:-

1. For a given mixing time, T , there is a wide range of the root mean square velocity gradient, G , that gives good performance. Also, extended mixing at optimum G , G_{opt} , gives improved performance (figures 4.1 to 4.4).
2. G_{opt} is inversely proportional to the logarithm of raw water turbidity and ranged from: 39 sec.⁻¹ to 15 sec.⁻¹ at 10°C; 29 sec.⁻¹ to 10 sec.⁻¹ at 20°C; and 19 sec.⁻¹ to 8 sec.⁻¹ at 30°C in the turbidity range 30 NTU to 1,200 NTU.
3. The optimum power function, $G_{opt} \cdot T_{opt}$, is also inversely proportional to the logarithm of raw water turbidity and ranged from: 22,250 to 4,950 at 10°C; 9,500 to 2,500 at 20°C; and 6,270 to 1,440 at 30°C in the turbidity range 30 NTU to 1,200 NTU. The variation is however much higher at 10°C than at 20°C or 30°C.
4. Temperature notably affected the efficiency of flocculation process i.e. lower temperatures require higher power input for a given performance; this effect is bigger at lower turbidity: at 10°C, 20°C, and 30°C, the $G_{opt} \cdot T_{opt}$ values were 22,250,

9,500, and 6,270 respectively for turbidity of 30 NTU and 4,950, 2,500, and 1,440 respectively for turbidity of 1,200 NTU implying that bigger flexibility in design is required at lower turbidity.

5. At higher turbidity, external mixing becomes less significant as mixing by differential settling predominates; no power input was required when raw water turbidity was greater than 4,000 NTU.
6. The logarithm of G_{opt} is proportional to the logarithm of T_{opt} and this relationship was independent of temperature or raw water turbidity.
7. The optimum G and T values obtained (8 to 38 sec^{-1} and 3 to 10 minutes) are small compared to recommended values in practice (5 to 100 sec^{-1} and 10 to 60 minutes).

The knowledge of quantitative relationships between the optimum flocculation parameters and the physical parameters of raw water quality provide guidance in the optimum design and operation of flocculation units.

5.2 Recommendations

Though the results of this study provide guidance for the optimum design and operation of flocculation units, some basic concerns still require additional study:-

1. Given that for a given T there is a wide range of G values that gives good performance and that extended mixing at optimum G gives improved performance, a convenient range of operation for an optimum design should be determined in terms of the physical

quality of water to make the optimum operation of flocculators less rigorous.

2. The possibility of after-floc problems resulting from short mixing period should be evaluated.

REFERENCES

1. Alaerts G. and Van Haute A., "Flocculation of Brackish Water From a Tidal River", Water Research Journal, Vol. 15, May, 1981, pp 517-523.
2. Argaman Y. A., "Pilot Plant Studies of Flocculation", JAWWA, Vol, 63, No. 12, Dec., 1971, pp 775-777.
3. Argaman Y. and Kaufman W. J., "Turbulence and Flocculation", Journal of San. Eng., ASCE, Vol. 96, No. SA 2, Apr. 1970, pp 223-241.
4. Argaman Y. and Kaufman W. J., "Turbulence in Orthokinetic Flocculation", Sanitary Engineering Research Laboratory Report No. 68-5, University of California, July 1968.
5. Black A. P. and Chen C., "Electrophoretic studies of Coagulation and Flocculation of River Sediment Suspensions with Aluminium Sulphate", JAWWA, Vol. 57, No. 3, Mar., 1965, pp 354-362.
6. Bratby J., Coagulation and Flocculation, Upland Press Ltd., England, 1980.
7. Camp T. R., "Floc Volume Concentration", JAWWA, Vol. 60, No. 6, June, 1968, p 656 - 673.
8. Camp T. R., Root D. A., and Bhoota B. V., "Effects of Temperature on Rate of Floc Formation", JAWWA, Vol. 32, Nov., 1940, pp 1913-1927.
9. Camp T. R. and Stein P. C., "Velocity Gradient and Internal Work in Fluid Motion", Journal, Boston Society of Civil Engineers, No. 30, 1943 pp 219-238.

10. Cleasby J. L., "Is Velocity Gradient a Valid Turbulent Flocculation Parameter?", Journal Env., Eng. ASCE, Vol. 110, No.5, Oct., 1984, pp 875-894.
11. Cochram K. G. and Cox G. M., Experimental Design, First Indian Edition, Asia Publishing House, Bombay, 1962. pp 26 - 28
12. Cox C. R., Operation and Control of Water Treatment Processes, W.H.O., Geneva, 1969, pp 54-78.
13. Dake J. M. K., Essentials of Engineering Hydraulics, 2nd Ed., The Macmillan Press Ltd., 1983, p 20.
14. Degremont, Water Treatment Handbook, A Halsted Press Book, John Wiley and Sons, New York, 1979.
15. Gloyna E. F. and Eckenfelder W. W. Jr., Water Quality Improvement by Physical and Chemical Processes III, University of Texas Press, 1970, pp 219-235.
16. Griffith J. D. and William R. G., "Application of Jar Test Analysis at Phoenix, Arizona", JAWWA, Vol. 64, No. 12, Dec., 1972, p 825.
17. Jahn S. Al Azharia, Traditional Water Purification in Tropical Developing Countries, Deutsche Gesellschaft Für Technische Zusammenarbeit (GTZ) GmbH, Fed. Rep. of Germany, 1981, pp 31-43, 135-188.
18. Jeffcoat W. B. and Singley J. E., "The Effect of Alum Concentration and Chemical Addition Time on Coagulation", JAWWA, Vol. 67, No. 4, Apr., 1975, pp 177-181.
19. Kawamura S., "Coagulation Considerations", JAWWA, Vol. 65, No.6, Jun., 1973, pp 417-423.

20. Mark M. C., "Critique of Camp and Stein's RMS Velocity Gradient", Journal Env. Eng. ASCE, Vol. III, No. 61, Dec., 1985, pp 741-754.
21. McCooke N. J. and West J. R., "The Coagulation of Kaolinite Suspension with Aluminium Sulphate", Water Research Journal, Vol. 12, Oct., 1978, pp 793-798.
22. Mhaishalkar V. A., Paramasivam R., and Bhole A. G., "Optimizing Physical Parameters of Rapid Mix Design for Coagulation-Flocculation of Turbid Waters", Water Research Journal, Vol. 25, No. 1, 1991, pp 43-52.
23. Montgomery J. M. Consulting Engineers, Inc., Water Treatment Principles and Design, John Wiley and Sons, 1985, pp 128-131, 514-517.
24. Morris J. K. and Knocke W. R., "Temperature Effects on the Use of Metal-ion Coagulants for Water Treatment", JAWWA, Vol. 76, Mar. 1984, pp 74-79.
25. Odira P. M. A. A., Upflow Filters in Flocculation and Direct Filtration of Waters of High Turbidity, Ph.D thesis, Tampere University of Technology, 1985 pp 44-58.
26. Parker D. S., Kaufman W. J., and Jenkins D., "Floc Breakup in Turbulent Flocculation Process", Journal San. Eng., ASCE, Vol. 98, No.SA1, Feb., 1972, pp 79-99.
27. Peavy H. S., Rowe D. R., and Tchobanoglous G., Environmental Engineering, McGraw Hill Book Company, Inc., New York, 1988, pp 131-151, 397.
28. Rafael A. V. and Letterman R. D., "Optimizing Flocculator Power Input", Journal, ASCE, Vol. 102, No. EE2, Apr., 1976, pp 251-263.

29. Reynolds A. J., Turbulent Flows in Engineering, John Wiley & Sons, London, 1974, pp 5, 394-402.
30. Treweek G. P., "Optimization of Flocculation Time Prior to Direct Filtration", JAWWA, Vol. 71, Feb., 1979, pp 96-101.
31. Von Smoluchowski M., "Trial of a Mathematical Theory of the Coagulation Kinetics of Colloidal Solutions, Journal, Physical Chemistry, No. 92, 1918, pp 129-155.
32. Walker R., Water Supply, Treatment and Distribution, Prentice-Hall, Inc., New Jersey, 1978, pp 148-154.
33. Water Treatment Plant Design, AWWA, Inc., Publication, New York, N.Y., 1969.

APPENDIX 1

DATA FROM THE FINAL EXPERIMENTS

The experimental data are presented in Tables A1-1 to A1-4 below.

A1-1. Results for Raw Water Turbidity of 30 NTU

- . Alum dose, $X = 20 \text{ mg/l}$ [Appendix 2]
- . NaHCO_3 dose, $Y = 45 \text{ mg/l}$ [Appendix 2]
- . Final pH $= 6.98$ [Appendix 2]

Table A1-1a: Results for water temperature of 10°C .

i	T = 15min.	G	30	40	50	60
		N	3.8	2.2	2.5	3.0
		G _{opt.}	40			

ii	G = 40s ₋₁	T	7	10	12	15
		N	3.7	2.6	2.2	2.0
		T _{opt.}	10			

iii	T = 10min.	G	35	40	45	50
		N	3.1	2.5	2.5	2.6
		G _{opt.}	40			

Table A1-1b: Results for water temperature of 20°C

i	T = 10min.	G	20	30	40	50
		N	3.0	1.7	1.8	2.0
		G _{opt.}	30			

ii	G = 30s ⁻¹	T	3	5	8	10
		N	3.8	2.4	2.0	1.8
		T _{opt.}	5			

iii	T = 5min.	G	25	30	35	40
		N	3.1	2.6	2.1	2.2
		G _{opt.}	30			

Table A1-1c: Results for Water Temperature of 30°C

i	T = 10min.	G	10	20	30	40
		N	3.8	1.9	1.6	1.6
		G _{opt.}	20			

ii	$G = 20s^{-1}$	T	3	5	8	10
		N	5.2	2.6	2.0	1.6
		$T_{opt.}$	5.5			

iii	$T = 5.5min.$	G	15	20	25	30
		N	3.3	2.3	1.9	1.6
		$G_{opt.}$	19			

A1-2: Results for raw water turbidity of 120 NTU

- . Alum dose, $X = 30 \text{ mg/l}$ [Appendix 2]
- . $NaHCO_3$ dose, $Y = 70 \text{ mg/l}$ [Appendix 2]
- . Final pH $= 7.02$ [Appendix 2]

Table A1-2 a: Results for water temperature of $10^{\circ}C$.

i	$T = 10min.$	G	20	30	40	50
		N	3.1	2.3	2.1	1.8
		$G_{opt.}$	30			

ii	$G = 30s^{-1}$	T	4	6	8	10
		N	4.0	3.0	2.3	2.0
		$T_{opt.}$	7			

iii	$T = 7min.$	G	25	30	35	40
		N	3.4	2.2	2.0	1.8
		$G_{opt.}$	28			

iv	$G = 28s^{-1}$	T	5	6	7	8
		N	4.3	3.2	2.5	2.5
		$T_{opt.}$	7.5			

Table A1-2 b: Results for water temperature of 20°C.

i	$T = 10min.$	G	10	20	30	40
		N	3.4	2.2	1.5	1.7
		$G_{opt.}$	20			

ii	$G = 20s^{-1}$	T	4	6	8	10
		N	3.7	2.6	2.3	1.9
		$T_{opt.}$	6			

iii	T = 6min.	G	15	20	25	30
		N	3.6	2.5	2.1	1.7
		G _{opt.}	20			

Table A1-2 c: Results for water temperature of 30°C.

i	T = 7min.	G	10	15	20	25
		N	3.5	2.2	2.0	1.6
		G _{opt.}	15			

ii	G = 15s ⁻¹	T	4	5	6	7
		N	2.8	2.6	2.2	2.2
		T _{opt.}	5			

iii	T = 5min.	G	10	15	20	25
		N	3.5	2.7	2.0	2.1
		G _{opt.}	15			

A1-3: Results for Raw Water Turbidity of 500 NTU.

- . Alum dose, $X = 120 \text{ mg/l}$ [Appendix 2]
- . NaHCO_3 dose, $Y = 300 \text{ mg/l}$ [Appendix 2]
- . Final pH $= 7.01$ [Appendix 2]

Table A1-3 a: Results for water temperature of 10°C .

i	T = 10min.	G	10	20	25	30
		N	4.8	2.2	2.0	1.6
		$G_{\text{opt.}}$	20			

ii	$G = 20\text{s}^{-1}$	T	4	6	8	10
		N	7.2	3.2	2.6	2.2
		$T_{\text{opt.}}$	8			

iii	T = 8min.	G	15	20	25	30
		N	3.0	2.4	2.1	1.5
		$G_{\text{opt.}}$	20			

Table A1-3 b: Results for water temperature of 20°C .

i	T = 5min.	G	10	20	25	30
		N	3.1	1.9	1.7	1.8
		$G_{\text{opt.}}$	20			

ii	$G = 20s^{-1}$	T	2	3	4	5
		N	18.6	3.9	2.8	2.1
		$T_{opt.}$	4.5			

iii	$T = 4.5min.$	G	10	15	20	25
		N	2.9	2.3	2.0	1.6
		$G_{opt.}$	15			

iv	$G = 15s^{-1}$	T	3	4	5	6
		N	16.1	3.3	2.5	1.9
		$T_{opt.}$	5			

Table A1-3 c: Results for water temperature of 30°C.

i	$T = 5min.$	G	10	15	20	25
		N	2.3	2.0	1.5	1.3
		$G_{opt.}$	10			

ii	$G = 10s^{-1}$	T	2	3	4	5
		N	10	3.7	2.6	2.1
		$T_{opt.}$	4			

iii	G	5	8	10	12.5
	N	10.7	4.6	2.4	2.2
	$G_{opt.}$	10.5			

A1-4: Results for Raw Water Turbidity of 1200 NTU.

- . Alum dose, $X = 275 \text{ mg/l}$ [Appendix 2]
- . NaHCO_3 dose, $Y = 600 \text{ mg/l}$ [Appendix 2]
- . Final pH $= 7.0$ [Appendix 2]

Table A1-4 a: Results for water temperature of 10°C .

i	G	10	20	25	30
	N	2.9	1.8	1.5	1.6
	$G_{opt.}$	20			

ii	T	5	6	7	8
	N	2.1	2.2	1.9	1.7
	$T_{opt.}$	5			

iii	T = 5min.	G	10	12.5	15	20
		N	8.7	3.2	2.6	2.0
		G _{opt.}	15			

iv	G = 15s ⁻¹	T	3	4	5	6
		N	12.3	4.0	2.5	2.4
		T _{opt.}	5.5			

Table A1-4 b: Results for water temperature of 20°C.

i	T = 5min.	G	10	15	20	25
		N	2.0	1.6	1.4	1.0
		G _{opt.}	10			

ii	G = 10s ⁻¹	T	2	3	4	5
		N	6.8	2.9	2.2	1.8
		T _{opt.}	3.5			

iii	T = 3.5min.	G	5	8	10	12.5
		N	13.5	3.3	2.4	2.2
		G _{opt.}	10			

Table A1-4 c: Results for water temperature of 30°C.

i	T = 5min.	G	5	8	10	12.5
		N	3.8	2.1	1.5	0.9
		G _{opt.}	8			

ii	G = 8s ⁻¹	T	2	3	4	5
		N	3.0	2.4	2.3	1.9
		T _{opt.}	3			

iii	T = 3min.	G	5	8	10	12.5
		N	10.8	2.2	1.2	0.8
		G _{opt.}	8			

APPENDIX 2

RESULTS OF PRELIMINARY EXPERIMENTS

A2-1. Optimum Coagulant Dose.

The optimization results are in Tables A2-1 below and in the corresponding Fig.A2-1. Sodium bicarbonate dose, Y (mg/l), was fixed at half the turbidity value in each case.

Table A2-1 a: Results for raw water turbidity of 30 NTU at 10°C.

Alum dose, X(mg/l)	5	10	20	30
Res. turbidity, N(NTU)	8.5	3.7	2.5	2.4
Optimum dose (mg/l)	20			

Table A2-1 b: Results for raw water turbidity of 120 NTU at 10°C.

Alum dose, X(mg/l)	20	30	40	50
Res. turbidity, N(NTU)	2.8	1.6	1.6	1.7
Optimum dose (mg/l)	30			

Table A2-1 c: Results for raw water turbidity of 500 NTU at 10°C.

Alum dose, X(mg/l)	80	100	120	140
Res. turbidity, N(NTU)	16.6	3.9	2.2	2.0
Optimum dose (mg/l)	120			

Table A2-1 d: Results for raw water turbidity of 1200 NTU at 10°C.

Alum dose, X(mg/l)	250	275	300	325
Res. turbidity, N(NTU)	6.3	3.5	3.5	5.5
Optimum dose (mg/l)	275			

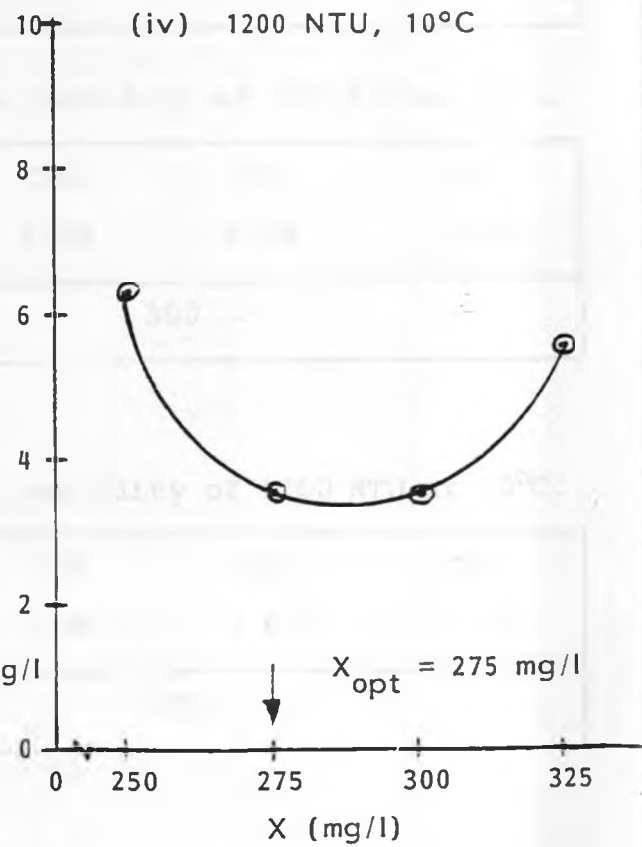
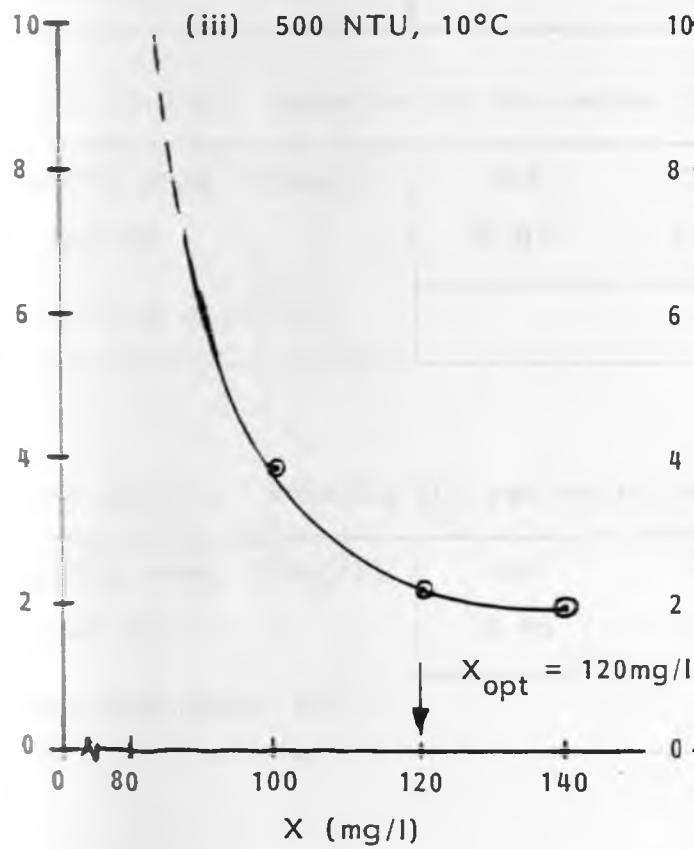
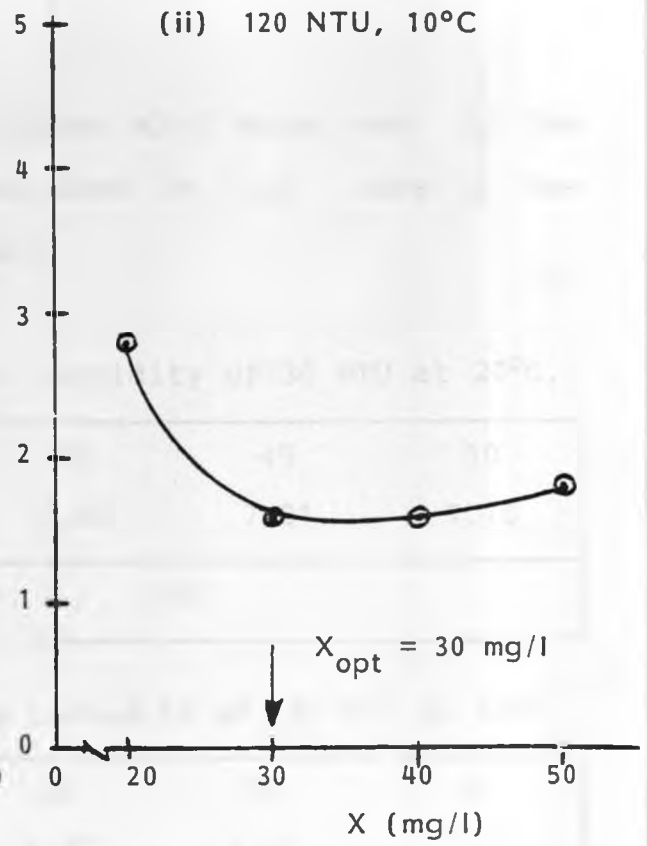
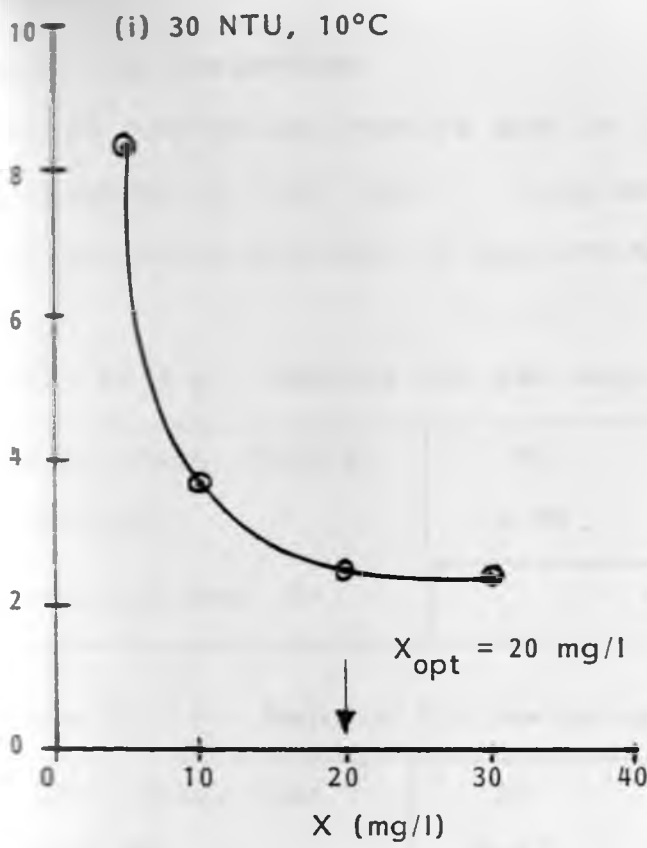


Fig. A2-1. Optimum Coagulant dose.

A2-2. pH Correction

The pH correction results are in Tables A2-2 below and in the corresponding Fig. A2-2. Coagulant dose in each case is the optimum value obtained in section A2-1.

Table A2-2 a: Results for raw water turbidity of 30 NTU at 20°C.

NaHCO ₃ dose, Y(mg/l)	35	40	45	50
Final pH	6.68	6.80	7.01	7.10
Required dose, Y*	45			

Table A2-2 b: Results for raw water turbidity of 120 NTU at 20°C.

NaHCO ₃ dose, Y(mg/l)	50	60	70	80
Final pH	6.67	6.87	7.03	7.17
Required dose, Y*	70			

Table A2-2 c: Results for raw water turbidity of 500 NTU at 20°C.

NaHCO ₃ dose, Y(mg/l)	200	250	300	350
Final pH	6.81	6.88	6.98	7.13
Required dose, Y*	300			

Table A2-2 d: Results for raw water turbidity of 1200 NTU at 20°C.

NaHCO ₃ dose, Y(mg/l)	400	500	600	700
Final pH	6.66	6.83	7.02	7.11
Required dose, Y*	600			

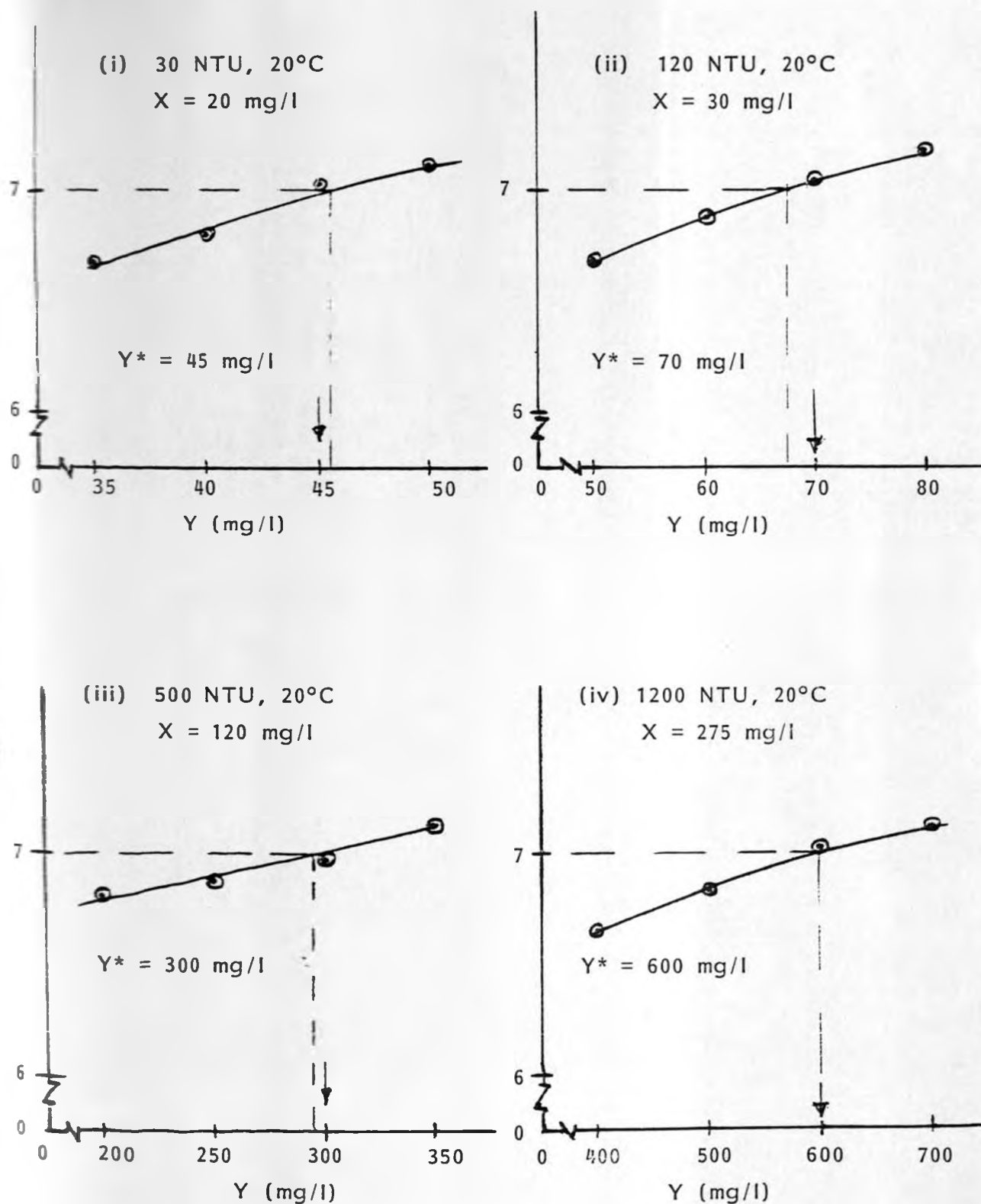


Fig. A2-2. Sodium bicarbonate dose for pH correction.